COVID-19 Spreading Prediction in a Control Room of Power Plant Using CFD Simulation

Shahram Karami
Hakim Sabzevari University
Esmail Lakzian (e.lakzian@hsu.ac.ir)
Hakim Sabzevari University https://orcid.org/0000-0002-7274-3554
Bok Jik Lee
Seoul National University
Majid Ebrahimi Warkiani
UTS: University of Technology Sydney
Omid Mahian
Xi'an Jiaotong University
Goodarz Ahmadi
Clarkson University

Research Article

Keywords: COVID-19, Control room, Power plant, Discrete Phase Model (DPM), Air curtain.

Posted Date: March 24th, 2022

DOI: https://doi.org/10.21203/rs.3.rs-1389314/v1

Abstract

Coughing and sneezing are the main ways of spreading coronavirus-2019 (SARS-CoV-2). Strategically critical facilities such as power plants cannot be shut down even in challenging situations like the COVID-19 outbreak. The personnel of the power plants' control room need to work together at close distances. This study presents the computational fluid dynamics (CFD) simulation results on the dispersion and transport of respiratory droplets emitted by an infected person coughs in a control room with an air ventilation system. This information would be helpful for risk assessment and for developing mitigation measures to prevent the spread of infection. The turbulent airflow in the control room is simulated using the k-ε model. The particle equation of motion included the drag, the Saffman lift, the Brownian, gravity/buoyancy, and thermophoresis forces. The simulation results showed that after 115 s, the cough droplets are dispersed in the entire room, and there is no safe (virus-free) space in the control room. Therefore, a safer design for the ventilation system is proposed by placing the ventilation air inlet and outlet registers across the control room and creating airflow patterns similar to air curtains that divided the room into three compartments.

1. Introduction

The coronavirus (SARS-CoV-2) spreads by exposure to respiratory droplets emitted by an infected person by breathing, speaking, coughing, and sneezing. On the other hand, strategic units such as power plants are critical facilities and need to stay functional during pandemics (Wahaj et al. 2022). Furthermore, the staff has to work at close distances in the control room of these power plants. Therefore, there are concerns in ensuring the safety and health of the control room personnel against uncertainties of the COVID-19 infection pathways. The critical questions that need to be addressed are how the existing HVAC systems affect the distribution of emitted droplets in the power plant's control room and how to minimize the chance for exposure. As the experimental study is not practical, computational fluid dynamics (CFD) provides a valuable tool to simulate the distribution and the spreading of virus-laden droplets generated by an infected person sneezing or coughing in a power plant control room. In particular, this study simulates the influence of air ventilation systems and room geometry on the spread of COVID-19 due to an infected person's coughs. In addition, the influence of dividing the control room into three parts with the use of a ventilation system that generates an air curtain-type flow pattern on the suppression of exposure to coronavirus (SARS-CoV-2) is studied. The world is now facing the Covid-19 pandemic; there have been some studies on the emergence of coronaviruses structures (Liu et al. 2021).

They examined the biology of the virus itself and the characteristics of the infection of a single human host. They studied the size, volume, and mass of the virus and found that the density of the virus is similar to water. Over the past years, several studies on the numerical prediction of transport of viruses (Particles generated from coughing or sneezing) have been reported in the literature (Bar et al. 2020). They examined the effect of dispersion of cough particles using the RNG k-ε turbulence model approach. They found that the ambient temperature and humidity affect the particle evaporation rate and dispersion pattern (Li, X et al. 2018). They calculated a Markov chain model to predict transient transport of viruses

(Particles generated from coughing or sneezing) in closed environments employing the k-ε turbulence model (Chen, Y et al. 2020). They numerically investigated the human body's thermal plume effect on cough particles' evaporation and dispersion using the Eulerian-Lagrangian approach and the RNG k-ε turbulence model (Yan, Y et al. 2019). They used the RNG k-ε turbulence model and compared their numerical results with the earlier published works. They suggested that the RNG k-ε model predicted the airflows with reasonable accuracy in their simulations (Baker, N et al. 2020). They suggested that the RNG k-ε model is preferable to the standard k-ε model for indoor airflow simulation (Chen, Q et al. 1995). They simulated the evaporation and dispersion of sputum droplets expelled by human coughs or sneezes using the RNG k-ε turbulence model (Redrow et al. 2011). They investigated the pattern of airflow and particle dispersion in a cleanroom using the RNG k-ε turbulence model (Eslami et al. 2016). They used the RNG K-ε turbulence model to simulate the particle distribution and deposition in a ventilated room. They also validated their predicted particle concentrations by comparison with the experimental data and obtained acceptable results (Chen, F et al. 2006).

In recent decades, numerous studies have been conducted to understand the cough droplets' dispersion in enclosed spaces. They did a numerical analysis and examined the particle dispersion in a laboratory. The diameters of the droplets used are 0.6 and 0.7 μm, and the standard k-ε turbulence model was used to solve the airflow field (Liu, Z et al. 2020). They investigated the effectiveness of ventilation design strategies for general hospital wards for virus removal using the Eulerian-Lagrangian simulations method. Their results showed that the location of an infected patient would affect the infection risks to other occupants. In addition, an increased air change rate in the ward could reduce the risk of infection (Yu, H et al. 2017). They used a CFD method to study the transport characteristics of gaseous pollutants in a chemical laboratory under different ventilation conditions. They concluded that the source of pollution, ventilation mode, and air exchange rate significantly affect the overall exposure risk (Lu, W et al. 1996). They investigated the distribution trend of cough droplets released in high-speed rail cabins using CFD simulations. The cabin was occupied by 48 passengers with 12 rows and 4 columns. They also studied different boundary conditions for the air supply and the exhaust systems (Zhang, L et al. 2012). They examined the coughing flows considering wet conditions. They simulated the process of coughing as a turbulent jet/puff phenomenon (Diwan et al. 2020). They conducted numerical studies on suspended particle dispersion, droplet spread, and airborne particle transmission of SARS-CoV-2 in public places, including department stores. They employed the Eulerian-Lagrangian approach to track the drops with different diameter ranges from small (below 100 μm) to large droplets (above 200 μm) (Wuorinen et al. 2020). Finally, they investigated the effect of air on aerosol and reported that the pattern of air distribution is an essential factor in influencing the residence time of bio aerosols in the laboratory (Feng et al. 2019). They investigated the risk factors for the transmission of COVID-19 using data on mainland China. Gical factors may play important roles in the transmission of COVID-19 in mainland China and could be integrated into consideration by public health alarm systems to better prevent the disease. The results indicate that warm area can also be at higher risk of the disease with the increasing wind speed (Wei et al. 2020). They have done studies in ventilation conditions and their influence on thermal comfort in examination classrooms. Current evidence and recent publications have led to the recognition that

aerosol-borne transmission of COVID-19 is possible in indoor areas such as educational centers and a crucial measure to reduce the risk of infection in high occupancy indoors is ventilation. In situ measurements of the environmental variables were taken during different evaluation tests. These measures affected the thermal comfort of the occupants, especially when the outside temperature was below 6°C (Miranda et al. 2021). They investigated the one-dimensional droplet evaporation model. Four initial droplet diameters (0.001, 0.01, 0.1, and 1 mm), two ambient temperatures (20 and 30 ^{o} C), and a range of ambient relative humidity are considered. The results also suggest that there may exist a critical ambient relative humidity; beyond which, the droplet lifetime will increase exponentially. It must be mentioned that the results do not imply that the COVID-19 virus will be deactivated at the end of the droplet lifetime (Chen, L et al. 2020). They conducted a series of numerical studies on suspended droplet dispersion and spread of SARS-CoV-2 in a classroom. They employed the Eulerian-Lagrangian approach to track the droplets of different diameters from submicron to 150μm. Their results indicated that using seat partitions for individuals can prevent the infection from a speaker in the front of the class to a certain extent. In the absence of partitions, the closest seats to the infected person had the highest average droplet concentration (Mirzaie et al. 2021). They conducted numerical studies using computational fluid dynamics (CFD) for modeling droplet motion. They employed the Eulerian-Lagrangian approach to track the drops (Yazdani et al. 2020). They have performed numerical analysis and particle dispersion in the classroom. The results indicate the significant effect of air conditioning and open window close to the infected person in reducing environmental pathogens (Ahmadzadeh et al. 2021). They investigated the numerical analysis of COVID-19 detection and the vitality of emerging technologies and preventive measures to prevent particle dispersion. The results show that such a preventive measure to track and manage the outbreak of the disease is effective in the current and future outbreaks of diseases (Asif et al. 2021). They simulate the evaporation and dispersion of sputum droplets expelled by human coughs or sneezes. The numerical analysis with diameters between 1 and 250μm is investigated inside a bus. The results indicate the ventilation process is found to feature dual effects on the distribution of the droplets. Simple increases in the ventilation rate may accelerate the droplets transmission (Mesgarpour et al. 2021). They have done studies on masks because wearing a mask is essential for human safety from this virus. Investigated the recycling of mask materials for addressing the environmental problems and transforming as a high value-added material through chemical modification of masks (Kim et al. 2022).

Air- curtains are typically formed by impinging plane jets used to separate two environments in terms of heat and mass transfer while still allowing traffic between these environments. The many applications of air curtains across a wide variety of industries evaluate their performance an important task. Recently, there have been several studies on the performance of air curtains in indoor environments. They examined the influence of an air curtain in a fully mechanized Industrial space. They also performed field measurements to validate the accuracy of their simulation results. Their findings showed that the CFD approach accurately describes the airflow field and dust distribution in a fully-mechanized excavation face with air curtains (Yu, H et al. 2017). They focused on characterizing the non-uniform air curtain in the dual-temperature open display cabinets. They used an experimentally validated 3-dimensional CFD

model in their simulations. Their results facilitated the development of more efficient air curtains for supermarket and convenience stores applications (Wang, Y et al. 2021). In their paper, they investigated the thermal effectiveness of the air curtains in stadiums. They modeled the thermal conditions and included the effect of solar irradiance on the interior and exterior surfaces. Their models are conducted for the stadium with and without air curtain gates and roof cooling to evaluate their thermal performance (Zhong, F et al. 2021).

The presented literature survey and the uncertainties surrounding the spreading of the COVID-19 suggest that more research on the transmission pattern of this virus in enclosed spaces such as the power plant's control room is needed. The present study uses CFD to simulate the spreading of droplets containing the COVID-19 virus expelled by coughing of an infective person standing in a power plant control room. The turbulent air flow is simulated using the k-ε turbulence model. The governing equations for the airflow and droplets are solved using the ANSYS-Fluent-20 software. The effects of ventilation airflow speed, droplet diameters, and creating air curtain-type flow patterns on the spreading of cough droplets are studied. Motion and concentration of COVID-19 infected droplets are evaluated using the three-dimensional Eulerian-Lagrangian simulations. This study examined how the virus-infected droplets spread and proposed a ventilation system that generates air curtain-type flow patterns as a solution for creating safe spaces. The simulation results showed that the aerosolized droplet distribution in the control room is not uniform and is strongly influenced by the air ventilation layout. Changing the ventilation inlets and outlets in the control room and creating an air curtain-type flow pattern in the control room significantly reduces virus-infected cough droplet dispersion and spreading.

2. Methodology

2.1. Physical model

Power plants are among the most significant and strategic places in a country, where people work in shifts at close distances. Therefore, the infection of one person can endanger the health of others. Figure 1 shows the geometry of the studied power plant control room. The room dimensions are 10 m × 6 m × 3 m, with the capacity of ten staff members working simultaneously. Figure 1 also shows the $1 \times 0.5\ m^2$ ventilation inlet and outlet registers in the control room.

As noted before, using an air curtain could lead to significant savings in building energy usage. In addition, the air curtains could also prevent the spread of respiratory droplets in indoor environments and provide a suitable non-obstructive solution for mitigation measures to prevent the spread of infection. Figure 2 shows the two ventilation flow patterns, including one along the length of the control room and the other across the control room.

Figure 2 indicates two ventilation cases studied in the power plant's control room and a comparison of the two approaches. The ventilation system's primary airflow is along the length of the control room in case a and along the width of the control room (air curtain) in case b. Air change per hour (ACH) is how

many times the air in the room changed in each hour. The ACH is evaluated as the ratio of the ventilation air volume added to a room in one hour, divided by the volume of the room. In this study, a ventilation rate of ACH = 10.26 h^{-1} in cases 1 and 2 shown in Fig. 2 is used, so the amounts of inlet air for both ventilation systems are the same.

Figure 3 shows the virtual plane to divide the space (A1 to A15). The average droplet concentration after coughing of the infected person for each area at the height of 1.85 m (the height of the infected person).

Table 1
Different ventilation flow patterns in a 3D control room.

Case	Description	
1	The ventilation system along the length of the control room	Infected person in location A (See Fig. 2.) Infected person in location B (See Fig. 2.) Infected person in location C (See Fig. 2.) Three Infected persons in locations A, B, and C (See Fig. 2.)
2	The ventilation system along the width of the control room **(with air curtain-type flow pattern formation)**	Infected person in location A (See Fig. 2.) Infected person in location B (See Fig. 2.) Infected person in location C (See Fig. 2.) Three Infected persons in locations A, B, and C (See Fig. 2.)

Table 1 shows different ventilation flow patterns in the 3D control room. When an infected person is in one of the room sections (A, B, or C), the air curtain-type flow pattern reduces the respiratory droplet spreading (see Fig. 2).

2.2. Mathematical modeling

This study performs numerical modeling of the airflow dynamics in the control room and dispersion and transport of the COVID virus-infected droplets. First, the steady-state airflow condition in the control room is simulated. Then, airflow and various size respiratory droplets (potentially carrying COVID-19 viruses) are expelled by coughing from the infected person's mouth standing in the control room and tracked

using the Eulerian-Lagrangian method. The turbulent airflow was simulated using the k-ϵ model (Li, X et al. 2018). We consider a COVID-19 infected person (with a height of 1.85 m and mouth area of 4 cm^2) standing in the control room, coughing and expelling the virus-infected droplets into the environment (Diwan et al. 2020). It is assumed that the exhalation airflow temperature is 37° C, the cough airflow and droplets' injection velocity is 10 m/s, the time duration of a single cough is 0.75 s, and the ambient temperature is 25° C. The droplets dispersion simulations after their release by coughing are continued for about 115 s.

3. Governing Equations

The governing equations are presented in this section.

3.1. Ventilation airflow modeling

The general equations of conservation of mass, momentum, and energy for an incompressible airflow are given as:

$$\frac{\partial \rho}{\partial t} + \nabla \cdot \left(\rho \vec{V}\right) = 0 \quad (1)$$

$$\rho\left(\frac{\partial V}{\partial t} + \vec{V} \cdot \nabla \vec{V}\right) = -\nabla P + \mu \nabla^2 \vec{V} + \vec{S}_T \quad (2)$$

$$\rho \frac{\partial T}{\partial t} + \rho \vec{\nabla} \cdot \left(T \vec{V}\right) = \nabla \cdot \left(\frac{K}{C_p} \nabla T\right) + S_T \quad (3)$$

3.2. Turbulence modeling

The RNG k-ϵ turbulence model has been used extensively for simulating the airflow in indoor environments and was shown to be a suitable model (Shih et al. 1995). The corresponding transport equations for the turbulence kinetic energy k and dissipation rate ϵ are given as:

$$\frac{\partial}{\partial t}(\rho k) + \frac{\partial}{\partial x_i}\left(\rho k u_i\right) = \frac{\partial}{\partial x_j}\left[\alpha_k \mu_{eff} \frac{\partial k}{\partial x_j}\right] + G_k - \rho\epsilon + S_k \quad (4)$$

$$\frac{\partial}{\partial t}(\rho \epsilon) + \frac{\partial}{\partial x_i}\left(\rho \epsilon u_i\right) = \frac{\partial}{\partial x_j}\left[\alpha_\epsilon \mu_{eff} \frac{\partial \epsilon}{\partial x_j}\right] + C_{1\epsilon}\frac{\epsilon}{k}\left(G_k\right) - C_{2\epsilon}\rho\frac{\epsilon^2}{k} - R_\epsilon + S_\epsilon \quad (5)$$

Where G_k is the generation of turbulence kinetic energy due to the mean velocity gradient, S_ε and S_k are user-defined source terms, and R_ε is the source term from renormalization. In equations (4) and (5), α_k and α_ε are the effective inverse Prandtl numbers for the turbulence kinetic energy and dissipation rate, and $C_{1\epsilon}$ = 1.42 and $C_{2\epsilon}$ =1.68, are model constants.

3.3. Discrete phase modeling

In the present study, transient cough airflow simulations are conducted. Then, cough droplets are injected into the domain with the same instantaneous velocity of the cough airflow of 10 m/s. The trajectories of virus-carrying droplets are evaluated using Newton's second law in a Lagrangian framework (Wang, J et al. 2017; Li, Y et al. 2020):

$$\frac{dV_d}{dt} = F_D\left(V - V_d\right) + \frac{g(\rho_d - \rho)}{\rho_d} + F_L + F_B \quad (6)$$

Where F_L, F_B, and F_D are the Saffman lift force, Brownian force, and drag force coefficient, respectively (Li et al. 1992). These are,

$$\boldsymbol{F_D = \frac{18\mu}{d^2 \rho_d C_C}} \quad (7)$$

$$C_C = 1 + \frac{2K}{d}\left(1.257 + 0.4e^{-\left(\frac{1.1d}{2K}\right)}\right) \quad (8)$$

Here C_C is the Cunningham coefficient (Chen, Y et al. 2017; Zhang, C et al. 2019).

The mass flow rate of droplets is given as:

$$\dot{m} = \frac{\left(\frac{4}{3}\pi r^3\right) \times \rho_d \times n)}{\bar{t}} \quad (9)$$

Where n and ρ_d are the number and density of particles, respectively.

The fraction of particles N_{Tn} remaining in space is given as,

$$N_{Tn} = \frac{N_t}{N_T} \times 100 \quad (10)$$

Where N_t ,N_T are particles remaining suspended at time t, and the total number of released particles, respectively.

4. Model Assumptions

To reduce the complexity of the simulation and to reduce the computational time, the following assumptions are made:

1- The droplets stick to surfaces without rebound after touching them.

2- The droplets collisions are neglected for dilute concentrations.

3- Cough emits airflow and droplets.

4- Temperature variations are negligible, and particle evaporation is ignored.

5- The physical properties of COVID-infected droplets are similar to water (Bar et al. 2020).

6- In these simulations, as shown in Table 3, the droplets are divided into six groups based on their diameter from 0.15 μm to 150 μm. For each diameter, 1800 droplets are released. That is, the total injection rate is 10,800 droplets per cough (Redrow et al. 2011).

4.1. Boundary conditions

The boundary conditions for solving the governing equations are shown in Table 2.

Table 2
Boundary conditions.

Boundary	Variable	Value	T(° C)
Inlet	Velocity inlet	3 m/s	17
Outlet	Pressure outlet	101 Pa	35
Wall	Velocity No-slip	0 m/s	Adiabatic
Person	Mouth inlet	10 m/s	37

4.2. Model validation

The present numerical model for simulation of the evaporation of a 10 μm droplet expelled by the coughing is validated by comparison with earlier results. It is assumed that the room humidity is 0%, droplets leave the mouth with a temperature of 37°C, and the room temperature is 25°C. The corresponding simulated diameter of a 10 μm droplet is then evaluated, and the results are shown in Fig. 4. This figure shows a good agreement between the present predictions and the results of (Li, X et al. 2018), with the differences less than 1%.

Figure 5 illustrates the validation of the airflow pattern in the three-dimensional two-zone room (Lu, W et al. 1996). The room (L × H × W = 5 m × 2.4 m × 3 m) is separated by a partition in the middle and a door in the centerline of the room. The width and height of the door are 0.7 and 0.95 meters, respectively. The thickness of the partition is ignored compared to the size of the room. A power supply and exhaust diffuser with length, width, and height of 1, 0.15, and 0.5 meters are located in the front and rear walls, respectively. The ventilation rate is ACH = 10.26 h^{-1}. The air velocity vector velocity patterns in the middle of the room (z = 1.5 m) are simulated, and the results are shown in Fig. 6 (a). Previous numerical study of (Lu, W et al. 1996) reproduced in Fig. 6 (b) for comparison. It is observed that the present prediction of the velocity field vector is in good agreement with (Lu, W et al. 1996).

5. Numerical Model

In this study, the RNG k-ε turbulence model is used, and the forces exerted on a respiratory droplet include theF_B, G, F_D, F_L, As noted before, the ANSYS-Fluent-20 software is used to simulate the airflow generated in the control room due to the ventilation system and the infected-person cough flow. They measured the flow rate, flow direction, and mouth opening area for 25 human subjects. The results of their study are used as boundary conditions in the present CFD simulations (Gupta et al. 2009). Accordingly, the infected person's mouth has a cross-section of 4 cm^2 (Diwan et al. 2020). The airflow rate during a cough is modeled as a combination of gamma functions. Then a user-defined function (UDF) is developed and used to generate the time variation of cough airflow rate at the mouth. Based on Table 3, cough particles are released into space simultaneously in six groups of diameters. For solving the governing equations, the finite volume method CFD software is used. The transient airflow is evaluated droplet tracking is

performed for the conditions listed in Table 3. The rate of convergence of 10^{-6} is considered to reduce the error in the iterations.

Table 3
Properties of simulated 6 diameter groups of respiratory droplets.

Case	d (μm)	$\dot{m}p$ (kg/s)	l_t (s)
1	0.150	4.24e-15	0.750
2	1	1.25e-12	0.750
3	10	1.25e-9	0.750
4	50	1.57e-7	0.750
5	100	1.25e-6	0.750
6	150	4.24e-6	0.750

5.1. Mesh and time independency

Meshing independence tests of the solution are presented in this section. Geometry cleanup has been carried out and checked for free edges, scar lines, duplicate surfaces, small fillets, holes, and intersection of parts. The computational domain is three-dimensional, and the computational mesh comprises of poly-hex core non-uniform structure. We have used edge and face sizing's for the human body and infected person to attain good mesh quality (in terms of skewness and orthogonal quality). Optimal and suitable meshes for simulation under steady and unsteady conditions are examined for speed and the mesh independence solution. Three meshes with 2,600,000, 3,200,000, and 3,400,000 cells are tested. Table 4 shows, the number of meshes and velocity average in domain solving flow. The average velocities predicted using the mesh with 3,200,000 cells differ less than 1% from those obtained by 3,400,000 cells. Finally, the mesh with 3,200,000 cells is selected for obtaining the mesh-independent simulations in the subsequent simulations.

Table 4
Grid-independence study in the control room.

N_m	V_A(m/s)
2,600,000	0.655
3,200,000	0.756
3,400,000	0.757
Figure 7. Mesh (poly-hexacore) structure used in the control room geometry.	

The resolution of 3,200,000 is sufficiently fine to capture the turbulent flow features in the control room (Fig. 7). In these simulations, y^+ less than 1. The time step size for the unsteady simulation is set at 0.005 s. The time-step independence tests showed that this time step size is sufficiently fine to capture the transient flow features. Reducing the time step from 0.005 did not show a noticeable change in the mean airflow velocity and mean droplet trajectories in the room. Therefore, a time step of 0.005 s is used to solve the time-dependent cases. Figure 7 shows the procedure of modeling the airflow and respiratory droplet transport in the power plant control room.

6. Results And Discussion

This paper investigates the dispersion and transport of respiratory droplets in the power plant's control room (with the operating ventilation system) for two scenarios:

• **Case 1** Effect of the infected person's distance from the ventilation system outlet on the spreading of emitted virus-infected droplets (Fig. 2a).

• **Case 2** Effect of the modified location of the ventilation air inlet and outlet in the control room to generate air curtain-type airflow patterns on the spreading of emitted virus-infected droplets (Fig. 2b).

Figure 8 (Case1) presents the velocity vector plots at the mid-planes of the inlet-outlet registers in the control room, including the cough airflows. The mean turbulent velocity vector fields under steady flow conditions are also shown in this figure. It is seen that the supply air forms a jet that extends across the room and creates a large circulating flow region. Figure 8 (Case2) shows the velocity vector plot in the control room and at the mid-planes of the modified ventilation inlet and outlet locations and cough emission from the infected-people mouths. It is seen that the ventilation airflow pattern changes significantly compared to case a, and airflow patterns similar to those of air curtains are generated. Figure 9 (Case1) shows the airflow streamlines emerging from the ventilation inlets. It is seen that the supply air forms a jet that extends across the room and creates a large circulating flow region. In addition, the streamlines starting from the cough airflows disperse in the control room, except for the person nearest to the outlet register. For this person, the cough airflow appears to leave the room through the outlet register. Figure 9 (Case2) shows the airflow streamlines starting from the ventilation inlets and cough emission from people's mouths in the control room with the modified ventilation system. It is seen that these streamlines mostly leave the room through the ventilation outlets.

The distributions of droplets of different sizes one second after coughing for the two ventilation systems are illustrated in Fig. 10. As noted before, coughing generates an airflow velocity of 10 m/s at the mouth for a duration of 0.75 s. As expected, droplets form a jet that is expelled from the mouth and follow the cough airflow. This figure shows that the distributions of different size droplets are quite similar after one second.

Figure 11 shows the respiratory droplet dispersion in the control room at different times for the two ventilation systems. The patterns of droplet dispersion in the control room are evaluated at different

times after the start of the cough. Here, the infected person in location A in the room coughs and expels droplets with diameters in the range of 0.15 μm to 150 μm. The following observations are made:

- At 1.5 s: Droplets form a jet that is expelled from the mouth and follow the cough airflow. The droplets start to spread near the mouth for both ventilation systems (Cases 1 and 2).
- At 20 s: Larger and heavier droplets tend to drop due to the gravitational force for both ventilation systems. But the smaller droplets (< 1 μm) remain suspended, and the ventilation airflow causes the smaller droplets to move towards the outlet.
- At 35 s: The differences in the droplet spreading in the room for the two ventilation systems become noticeable. The virus-infected droplets are in regions A and B of the room for the second ventilation system (Case 2), and there are a small number of droplets in region C. This is because the air curtain-type airflow patterns prevent the spread of virus-infected droplets in the control room. However, the droplets are spread in the entire room for the first ventilation system (Case 1).
- At 55 s: In Case 1 (first ventilation system), the droplets are spread all over the control room. However, in the Case 2 ventilation system, the cough droplets are mainly in regions A and B of the room, and there are only a small fraction of droplets in the C area. This is because the formation of air curtain-type airflow patterns in the room keeps the lightweight droplets in areas A and B while the ventilation air transports them towards the outlet register.
- At 75 s: In Case 1, the respiratory cough droplets are spread throughout the room and the droplet concentration is slowly reduced with time. However, in Case 2 (second ventilation system), almost all the droplets leave the control room.
- At 115 s (not shown here): Almost all droplets leave the room for the first ventilation system (Case 1) as well. However, as noted above in Case 2, at 75 s, there are no droplets in the control room. Therefore, it is concluded that the modified ventilation system (Case 2) is more effective in clearing the room from the emitted cough droplets compared to Case 1 ventilation system. This is due to the formation of air curtain-type flow patterns in the control room with the Case 2 ventilation system.

Figure 12 compares the cough droplet dispersion in the control room at different times for the two ventilation systems when the infected person is in region B of the room. The findings of Fig. 11 are as follows:

- At 1.5 s: Cough droplets form a jet from the mouth and follow the cough airflow. The droplets begin to spread in the face neighborhood for both ventilation systems (Cases 1 and 2).
- At 20 s: For both ventilation systems (Cases 1 and 2), the larger droplets tend to sediment due to gravity. However, the ventilation airflow transports the smaller droplets towards the outlet register.
- At 35 s: The dispersion of droplets in the control room slowly increases. It is observed that the droplet spreading differs in Cases 1 and 2. For the first ventilation system (Case 1), the droplets are distributed in the room. However, for the Case 2 ventilation system, the cough droplets are mainly in

regions B and C of the control room, with a small number in area A. As noted before, the formation of the air curtain-flow pattern prevents the spread of respiratory droplets in the room.

- At 55 s: In Case 1, the infected droplets are spread throughout the space. But in Case 2, the cough droplets are primarily in regions B and C of the room, with a small number in A. The air curtain-type flow patterns prevent the spread of virus-infected droplets in the room. Therefore, an appropriate design of the ventilation system of the control room could significantly reduce the spread of virus-infected droplets.
- At 75 s: In Case 1 ventilation system, the cough droplets are spread in the entire room, while their concentration gradually reduces with time. However, in Case 2 all cough droplets leave the room 75 s after the cough. Thus, the air curtain-type airflow patterns promote the removal of cough droplets.
- At 115 s (not shown here): All droplets leave the room for the first ventilation system (Case 1). However, as noted above, all droplets leave the room in Case 2 at 75 s. Therefore, the Case 2 ventilation system is more effective in removing the cough droplets from the room.

Figure 13 presents the simulation results for an infected person coughing in region C of the room and compares the dispersion patterns for the Cases 1 and 2 ventilation systems. The findings of Fig. 13 are:

- At 1.5 s: Emitted cough droplets form a jet expelled from the mouth that follows the cough airflow. At this time, the droplets spread slightly away from the mouth and are not affected by the Case 1 or Case 2 ventilation airflow.
- At 20 s: The larger and heavier droplets tend to drop faster due to the gravitational force for both ventilation systems. However, the smaller droplets remain suspended in the air move towards the outlet by the ventilation airflows. For Case 1, the cough droplets spread in regions B and C of the control room, while the droplets in Case 2 ventilations system remain in region C of the room.
- At 35 s: At this time, there are marked differences in the droplet spreading for the first and second ventilation systems. For the Case 1 ventilation system, the droplets are distributed in the control room. However, the cough droplets for the Case 2 ventilation system are in regions B and C of the room, with no droplets in the A area.
- At 55 s: In Case 1 ventilation system, the cough droplets are spread throughout the space. But in the Case 2 ventilation system, the virus-infected droplets are distributed mainly in regions B and C of the room with no virus-infected droplets in region A. The air curtain-type airflow patterns formed in Case 2 prevent the spread of droplets into area A.
- At 75 s: In Case 1 ventilation system, the virus-infected droplets spread all over the space, and the droplet concentration slowly reduces with time. In Case 2 ventilation system, however, 75 s after the cough, all droplets leave the room.
- At 90 s (not shown here): All droplets leave the room for the Case 1 ventilation system. However, as noted above, all droplets leave the room in Case 2 at 75 s. Therefore, the Case 2 ventilation system is more effective in removing the cough droplets from the room.

- Comparison of different cases shows that if the coughing person is near the outlet (location C), the droplet concentrations are slowly reduced in the area. On the contrary, if the coughing person is in the inner part of the room (locations A or B), the possibility that the virus-infected droplets disperse in the room is higher.

Figure 14 compares the time variation of droplets emitted by three infected persons at locations A, B, and C for the ventilations systems Cases 1 and 2. The findings of the results of Fig. 14 are as follows:

- At 1.5 s: Expelled cough droplets form three jets in front of the mouth of the emitters that follow their cough airflows. The droplets spread slightly away from the mouth due to the cough airflow, and they are not affected by the ventilation airflows.
- At 20 s: It is seen that the ventilation airflows move the lighter droplets towards the outlet registers. In Case 1 ventilation system, virus-infected droplets spread in the room, and their concentrations are gradually reduced in time. In Case 2 ventilation system, the air curtain-type airflow formations reduce the droplet dispersion and drive them more directly toward the outlet registers.
- At 35 s: Virus-infect droplets spreading increase in the area, while there are some differences between Cases 1 and 2 ventilation systems. For both ventilation systems, the droplets are scattered throughout the control room. However, for Case 2 ventilation systems, the droplets are more concentrated closer to the outlet registers.
- At 55 s: For Case 1, the whole room is still filled with cough droplets, and there is no safe space in the control room. In Case 2 ventilation system, the air curtain-type airflow patterns reduce the droplets spread across different regions. As a result, the cough droplets are concentrated mainly near the outlet registers, and the concentration on the inlet side of the room is relatively low.
- At 75 s: In Case 1 ventilation system, the virus-infected droplets are still spread all over the room, although at lower concentrations. However, in the Case 2 ventilation system, all cough droplets have left the room, and the entire control room is virus-free.
- At 115 s (not shown here): As is shown for the person coughing’s, all droplets leave the room for the first ventilation system (Case 1) 115 s after coughing. However, all droplets leave the room in Case 2 ventilation system 40 s earlier at 75 s. Therefore, as noted before, the Case 2 ventilation system is more effective in removing the cough droplets from the room.

Figure 15 shows the airflow streamlines for the two ventilation systems for coughing at different locations in the control room. This figure shows that in Case 1, the ventilation airflow causes the smaller cough droplets to move around the room before moving towards the outlet. Therefore, the possibility that the virus-infected droplets spread in the room is higher. The exception is for the person coughing in area C near the out. In this case, the streamline starting from the coughing person leaves direct from the outlet register. Therefore, the droplets' spread is smaller in the area. However, in Case 2, the formation of air curtain-type flow patterns reduces the cough droplet spreading. The air curtain-type airflow patterns create a non-obstructive barrier that reduces droplet dispersion substantially provides a mitigation measure to prevent the spread of infection.

Figure 16 and Fig. 17 present average droplet concentrations on the virtual plane (see Fig. 3) for the highest average droplet concentration area of each case at various times. The average droplet concentration of less than 10^{-16} kg/m^3 is considered negligibly small and is neglected.
Figure 18 shows time variations of the fraction of cough droplets remaining in the control room for different ventilation systems. When the ventilation airflow is along the length of the control room, it takes about 115 s for the cough droplets to leave space. However, when the ventilation air flow is across the width of the control room, it takes 75 s for the droplets to leave the room. For Case2, the formation of air curtain-type flow patterns reduces the spreading of droplets in the control room, and droplets move out faster through the outlet. For Case 1, when the coughing person is close to the outlet (location C), the emitted droplets quickly leave the room. Nevertheless, when the infected coughing person is far from the ventilation outlet (but close to the inlet) (location A), the cough droplets remain longer in the space.

7. Conclusions

A clear understanding of aerosol transport in different environments is crucial to developing physics-informed measures for COVID-19 spreading mitigation. This study investigates the dispersion of cough droplets in a realistic power plant's control room environment using CFD simulations. The simulation results showed that the aerosolized cough droplet distribution in the control room is not uniform and is strongly influenced by the air ventilation layout. The cough flow and droplet dispersion are investigated using the Eulerian-Lagrangian approach. Modifying the ventilation system in the control room to create air curtain-type airflow is also studied. Based on the simulation results, the following conclusions are drawn:

- For Case 1, when the ventilation airflow is along the control room's length, it takes about 115 s for the cough droplets to clear the room.
- For Case 2, the closer the coughing person to the ventilation outlet, the lower the droplets spread in the room.
- For Case 2, when the ventilation air flow is across the width of the control room, and there are air curtain-type airflow patterns in the room, it takes about 75 s for the cough droplets to clear the room.
- For Case 2, the air curtain-type airflow patterns reduce the spreading of droplets in space.
- **Case 2** ventilation system leads to the lower spread of droplets compared to Case 1 ventilation system.

Abbreviations

A	Surface area (m^2)
V_A	Velocity Average in domain solving flow (m/s)
C_C	Cunningham coefficient (-)
$C_{i,s}$	Vapor concentration at the Particle surface (kg mol/m^3)
$C_{i,\infty}$	Vapor concentration in the bulk gas (kg mol/m^3)
C_p	Specific heat capacity (J/kg K)
d	Particles diameter (μm)
$D_{i,m}$	Diffusion coefficient of vapor (m^2/s)
F_B	Brownian force (-)
F_D	Drag factor (-)
F_{TH}	Thermophoretic force (-)
F_L	Saffman lift force (-)
$\dot{m}_p$	Flow rate (kg/s)
G	Gravity (m/s^2)
g	Gravitational acceleration components (m/s^2)
h	Convective heat transfer coefficient (W/m^2-K)
h_{fg}	Latent heat (J/kg)
K	Fluid thermal conductivity (W/m K)
k_C	Mass transfer coefficient (m/s)
$M_{w,i}$	The molecular weight of species i (kg/kg mol)
m	Mass (kg)
N	Number of particles(-)
Nu	Nusselt number (hl/ka)
N_i	Molar flux of vapor (kg mol/m^2-s)
N_T	Total number of particles (-)
N_t	Particles at each time (-)
N_{Tn}	Particles remaining in space(-)
N_m	Number of meshes(-)
P	Pressure (Pa)
PRT	Particle Residence Time(s)
P_{op}	Operating pressure (pa)
R	Universal gas constant(J/kg.K)
Re	Reynolds number (-)
RH	Relative humidity (-)
P_{rt}	Particle Removal time(s)
m	Mass (kg)
S	Source term(C)
Sc	Schmidt number(-)
t	Time (s)
T	Temperature conditions (C)
u, v, w	Velocity components (m/s)
G_k, S_ε, S_k, α_k, α_ε	turbulent kinetic energy(-)
V_v	Ventilation velocity (m/s)
V	Velocity vector (m/s)
X, Y	Non-dimensional Cartesian coordinates (-)
Greek symbols	
α	Thermal diffusivity (m^2/s)
ε	Dissipation rate of the turbulent energy (-)
μ	Dynamic viscosity (m^2/s)
η	Particle removal efficiency (-)
ρ	Density (kg/m^3)
Subscripts	
sat	Saturation (-)
T	Total (-)
x,y, z	Cartesian directions (-)

Declarations

Ethics approval: This article does not contain any studies with human participants performed by any of the authors.

Consent to participate: We affirm that all authors have participated in the research work and are fully aware of ethical responsibilities.

Consent to publish: We affirm that all authors have agreed for submission of the paper to ESPR and are fully aware of ethical responsibilities.

Author contribution: Shahram Karami: Writing, Software, Simulation, Validation, Investigation. **Esmail Lakzian:** Methodology, Reviewing and Editing, Supervision. **Bok Jik Lee:** Reviewing and Editing. **Majid Ebrahimi Warkiani:** Reviewing and Editing. **Omid Mahian:** Reviewing and Editing.**Goodarz Ahmadi:** Reviewing and Editing, Supervision.

Funding: Not applicable.

Competing interests: The authors declare that they have no known competing financial interests or personal relationships that could have appeared to influence the work reported in this paper.

Availability of data and material: The data used in this manuscript is included in the text.

References

1. Ahmadzadeh, M., Farokhi, E., & Shams, M. (2021). Investigating the effect of air conditioning on the distribution and transmission of Covid-19 virus particles. Journal of Cleaner Production, 316, 128147.
2. Asif, M., Xu, Y., Xiao, F., & Sun, Y. (2021). Diagnosis of COVID-19, vitality of emerging technologies and preventive measures. Chemical Engineering Journal, 423, 130189.
3. Baker, N., Kelly, G., & O'Sullivan, P. D. (2020). A grid convergence index study of mesh style effect on the accuracy of the numerical results for an indoor airflow profile. International Journal of Ventilation, 19(4), 300-314.
4. Bar-On, Y. M., Flamholz, A., Phillips, R., & Milo, R. (2020). Science Forum: SARS-CoV-2 (COVID-19) by the numbers. Elife, 9, e57309.
5. Chen, F., Simon, C. M., & Lai, A. C. (2006). Modeling particle distribution and deposition in indoor environments with a new drift–flux model. Atmospheric Environment, 40(2), 357-367.
6. Chen, L. D. (2020). Effects of ambient temperature and humidity on droplet lifetime–A perspective of exhalation sneeze droplets with COVID-19 virus transmission. International Journal of Hygiene and Environmental Health, 229, 113568.
7. Chen, Q. (1995). Comparison of different k-ε models for indoor airflow computations. Numerical Heat Transfer, Part B Fundamentals, 28(3), 353-369.
8. Chen, Y., Liu, Q., & Guo, D. (2020). Emerging coronaviruses: genome structure, replication, and pathogenesis. Journal of medical virology, 92(4), 418-423.
9. Chen, Y. P., & Deng, Z. L. (2017). Hydrodynamics of a droplet passing through a microfluidic T-junction. J. Fluid Mech, 819, 401-434.
10. Diwan, S. S., Ravichandran, S., Govindarajan, R., & Narasimha, R. (2020). Understanding transmission dynamics of COVID-19-type infections by direct numerical simulations of cough/sneeze flows. Transactions of the Indian National Academy of Engineering, 5, 255-261.
11. Eslami, J., Abbassi, A., Saidi, M. H., & Bahrami, M. (2016). Effect of supply/exhaust diffuser configurations on the contaminant distribution in ultra-clean environments: Eulerian and Lagrangian approaches. Energy and Buildings, 127, 648-657.
12. Feng, X., Zhang, Y., Xu, Z., Song, D., Cao, G., & Liang, L. (2019). Aerosol containment by airflow in biosafety laboratories. Journal of Biosafety and Biosecurity, 1(1), 63-67.
13. Gupta, J. K., Lin, C. H., & Chen, Q. (2009). Flow dynamics and characterization of a cough. Indoor air, 19(6), 517-525.

14. Kim, S., Yang, X., Yang, K., Guo, H., Cho, M., Kim, Y. J., & Lee, Y. (2022). Recycling respirator masks to a high-value product: From COVID-19 prevention to highly efficient battery separator. Chemical Engineering Journal, 430, 132723.
15. Li, A., & Ahmadi, G. (1992). Dispersion and deposition of spherical particles from point sources in a turbulent channel flow. Aerosol science and technology, 16(4), 209-226.
16. Li, X., Shang, Y., Yan, Y., Yang, L., & Tu, J. (2018). Modelling of evaporation of cough droplets in inhomogeneous humidity fields using the multi-component Eulerian-Lagrangian approach. Building and Environment, 128, 68-76.
17. Li, Y. Y., Wang, J. X., & Chen, X. (2020). Can a toilet promote virus transmission? From a fluid dynamics perspective. Physics of Fluids, 32(6), 065107.
18. Liu, Z., Zhuang, W., Hu, L., Rong, R., Li, J., Ding, W., & Li, N. (2020). Experimental and numerical study of potential infection risks from exposure to bioaerosols in one BSL-3 laboratory. Building and Environment, 106991.
19. Liu, M., Li, Z., Liu, M., Zhu, Y., Liu, Y., Kuetche, M. W. N... & Tao, L. (2021). Association between temperature and COVID-19 transmission in 153 countries. Environmental Science and Pollution Research, 1-11.
20. Liu, W., Liu, D., & Gao, N. (2017). CFD study on gaseous pollutant transmission characteristics under different ventilation strategies in a typical chemical laboratory. Building and Environment, 126, 238-251.
21. Lu, W., Howarth, A.T., Adam, N. and Riffat, S.B., 1996. Modelling and measurement of airflow and aerosol particle distribution in a ventilated two-zone chamber. Building and environment, 31, 417-423.
22. Gupta, J. K., Lin, C. H., & Chen, Q. (2009). Flow dynamics and characterization of a cough. Indoor air, 19(6), 517-525.
23. Mesgarpour, M., Abad, J. M. N., Alizadeh, R., Wongwises, S., Doranehgard, M. H., Jowkar, S., & Karimi, N. (2021). Predicting the effects of environmental parameters on the spatio-temporal distribution of the droplets carrying coronavirus in public transport-A machine learning approach. Chemical Engineering Journal, 132761.
24. Miranda, M. T., Romero, P., Valero-Amaro, V., Arranz, J. I., & Montero, I. (2021). Ventilation conditions and their influence on thermal comfort in examination classrooms in times of COVID-19. A case study in a Spanish area with Mediterranean climate. International Journal of Hygiene and Environmental Health, 113910.
25. Mirzaie, M., Lakzian, E., Khan, A., Warkiani, M. E., Mahian, O., & Ahmadi, G. (2021). COVID-19 spread in a classroom equipped with partition–A CFD approach. Journal of Hazardous Materials, 420, 126587.
26. Redrow, J., Mao, S., Celik, I., Posada, J. A., & Feng, Z. G. (2011). Modeling the evaporation and dispersion of airborne sputum droplets expelled from a human cough. Building and Environment, 46(10), 2042-2051.

27. Shih, T. H., Liou, W. W., Shabbir, A., Yang, Z., & Zhu, J. (1995). A new k-ε eddy viscosity model for high Reynolds number turbulent flows. Computers & fluids, 24(3), 227-238.
28. Vuorinen, V., Aarnio, M., Alava, M., Alopaeus, V., Atanasova, N., Auvinen, M., & Österberg, M. (2020). Modeling aerosol transport and virus exposure with numerical simulations in relation to SARS-CoV-2 transmission by inhalation indoors. Safety Science, 130, 104866.
29. Wang, J., Sun, L., Zou, M., Gao, W., Liu, C., Shang, L., & Zhao, Y.(2017). Bioinspired shape-memory graphene film with tunable wettability. Science advances, 3(6), e1700004.
30. Wang, Y., Qian, S., Xu, J., Li, L., Dou, X., Li, X., ... & Yu, J. (2021). Numerical study on the air curtain characteristics of a dual-temperature open display cabinet. International Journal of Refrigeration, 126, 23-34.
31. Wahaj, Z., Alam, M., & Al-Amin, A. Q. (2022). Climate change and COVID-19: shared challenges, divergent perspectives, and proposed collaborative solutions. Environmental Science and Pollution Research, 1-10.
32. Wei, J. T., Liu, Y. X., Zhu, Y. C., Qian, J., Ye, R. Z., Li, C. Y., ... & Cheeloo EcoHealth Consortium. (2020). Impacts of transportation and meteorological factors on the transmission of COVID-19. International journal of hygiene and environmental health, 230, 113610.
33. Yazdani, S., & Lakzian, E. (2020). Numerical simulation and passive control of condensing flow through turbine blade by NVD Method Using Eulerian–Lagrangian Model. Computers & Mathematics with Applications, 80(1), 140-160.
34. Yan, Y., Li, X., & Tu, J. (2019). Thermal effect of the human body on cough droplets evaporation and dispersion in an enclosed space. Building and Environment, 148, 96-106.
35. Yu, H., Cheng, W., Wang, H., Peng, H., & Xie, Y. (2017). Formation mechanisms of a dust-removal air curtain in a fully-mechanized excavation face and an analysis of its dust-removal performances based on CFD and DEM. Advanced Powder Technology, 28(11), 2830-2847.
36. Yu, H. C., Mui, K. W., Wong, L. T., & Chu, H. S. (2017). Ventilation of general hospital wards for mitigating infection risks of three kinds of viruses including Middle East respiratory syndrome coronavirus. Indoor and Built Environment, 26(4), 514-527.
37. Zhang, C., Wu, S., & Yao, F. (2019). Evaporation regimes in an enclosed narrow space. International Journal of Heat and Mass Transfer, 138, 1042-1053.
38. Zhang, L., & Li, Y. (2012). Dispersion of coughed droplets in a fully-occupied high-speed rail cabin. Building and Environment, 47, 58-66.
39. Zhong, F., Chaudhry, H. N., & Calautit, J. K. (2021). Effect of Roof Cooling and Air Curtain Gates on Thermal and Wind Conditions in Stadiums for Hot Climates. Energies, 14(13), 3941.

Figures

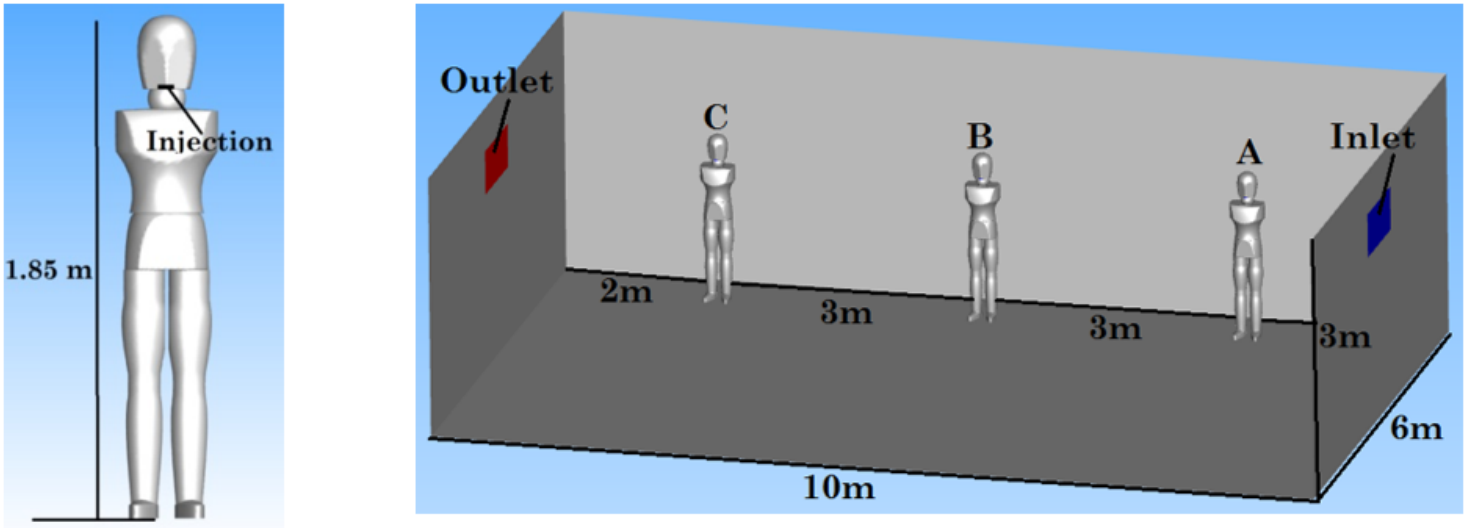

Figure 1

The geometry of the power plant control room and mannequins.

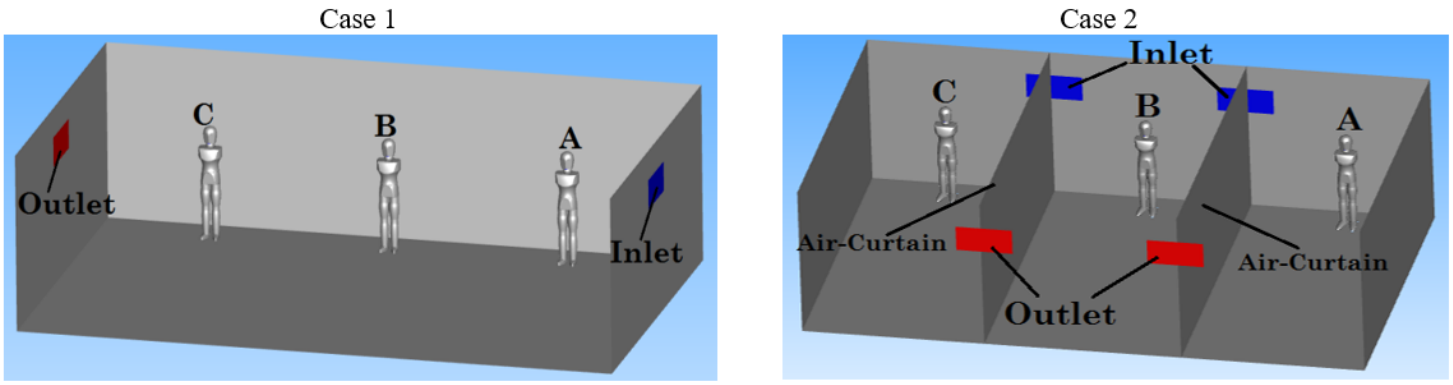

a) Ventilation airflow along the length of the control room. b) Ventilation airflow across the width of the control room.

Figure 2

The geometry of the ventilation airflow pattern in the control room.

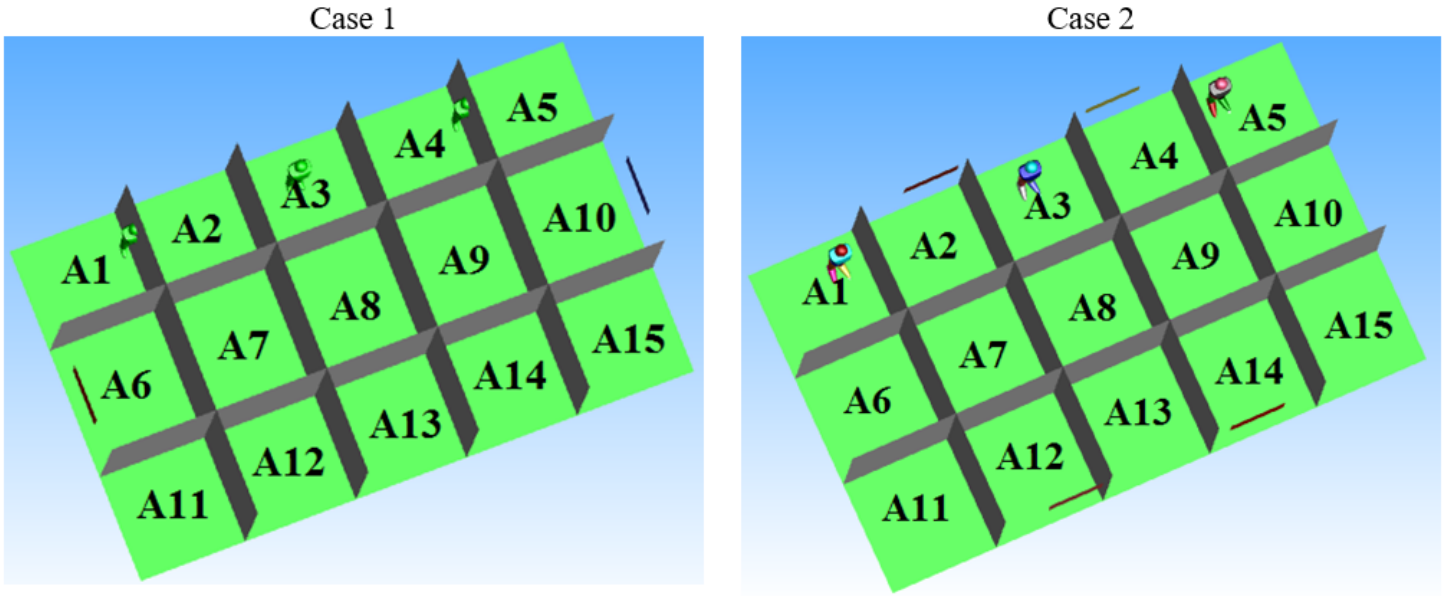

Figure 3

Schematic of the control room from the top view.

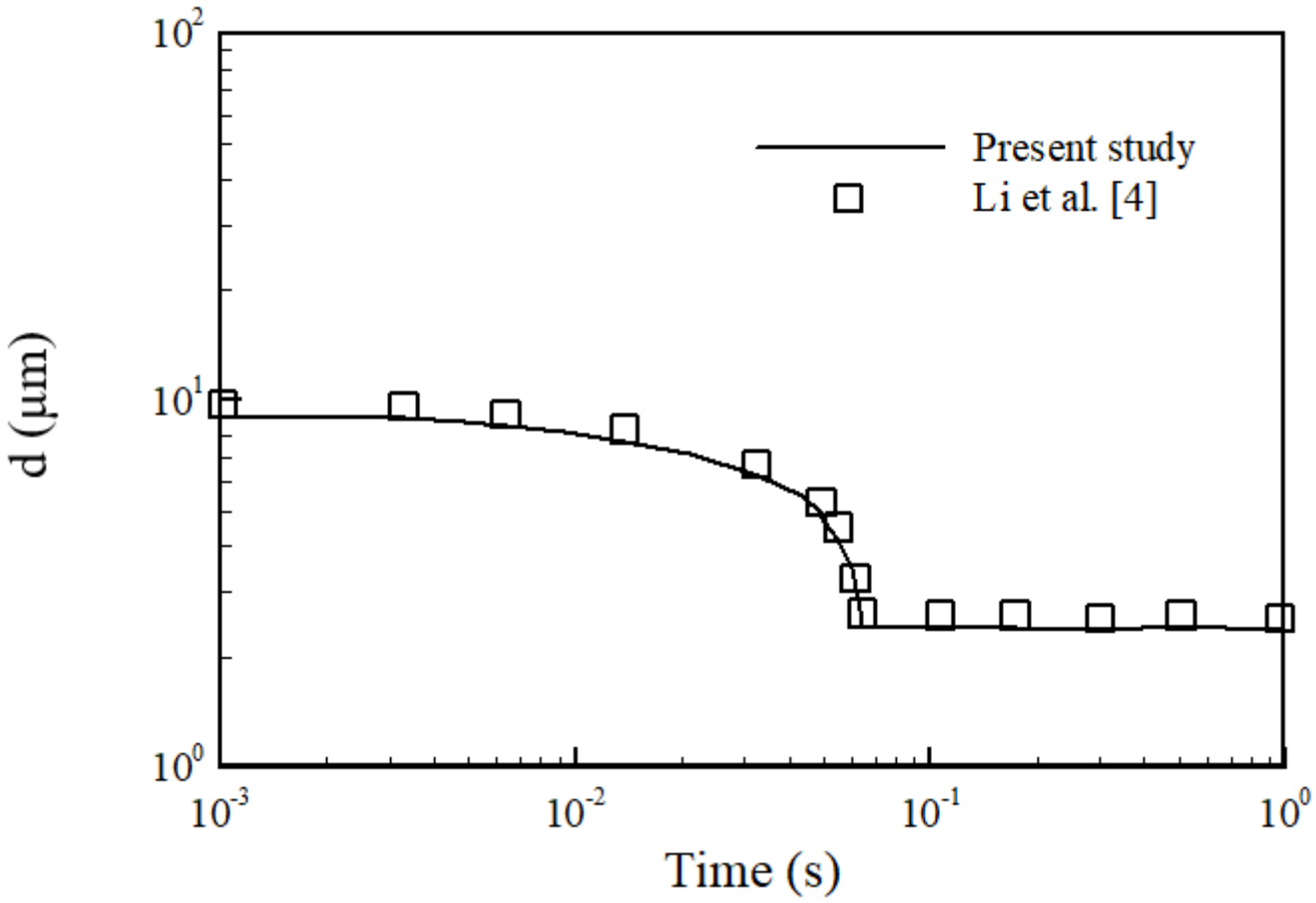

Figure 4

Comparison of the present study for evaporation of a 10 μm droplet with (Li, X et al. 2018).

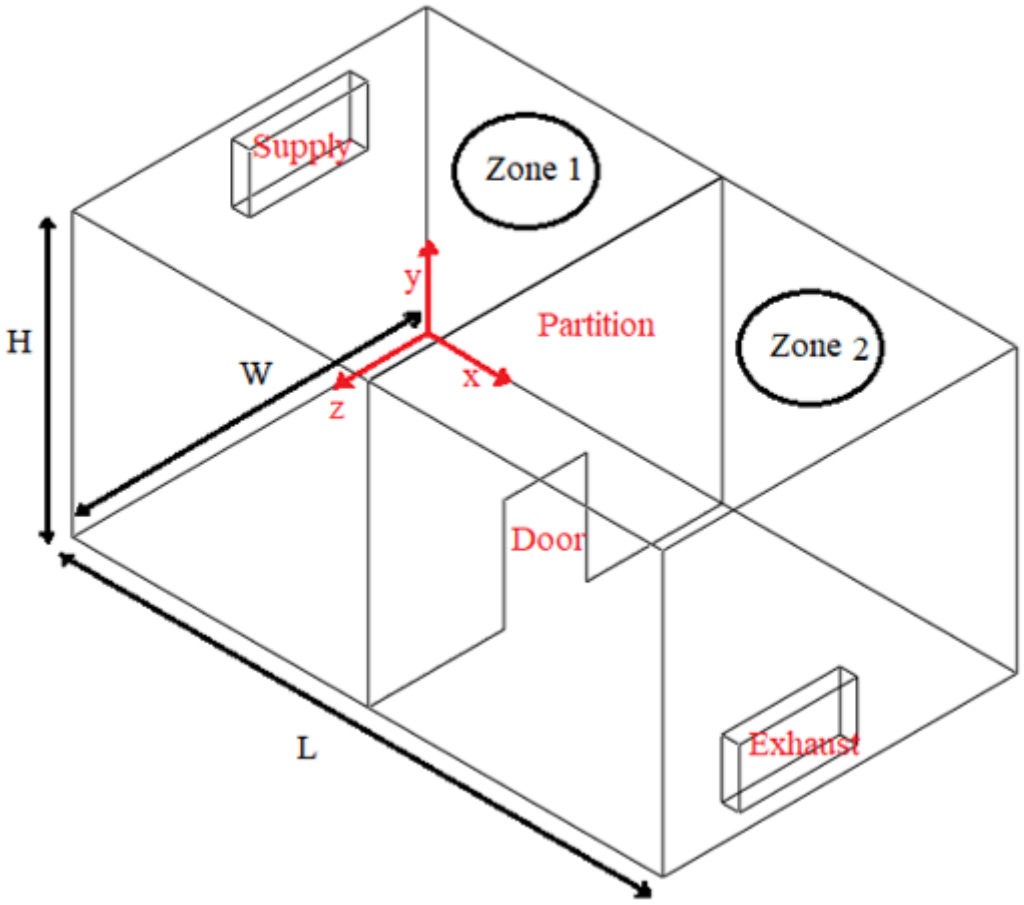

Figure 5

The Schematic of the 3-dimensional two-zone room (Li et al. 1992).

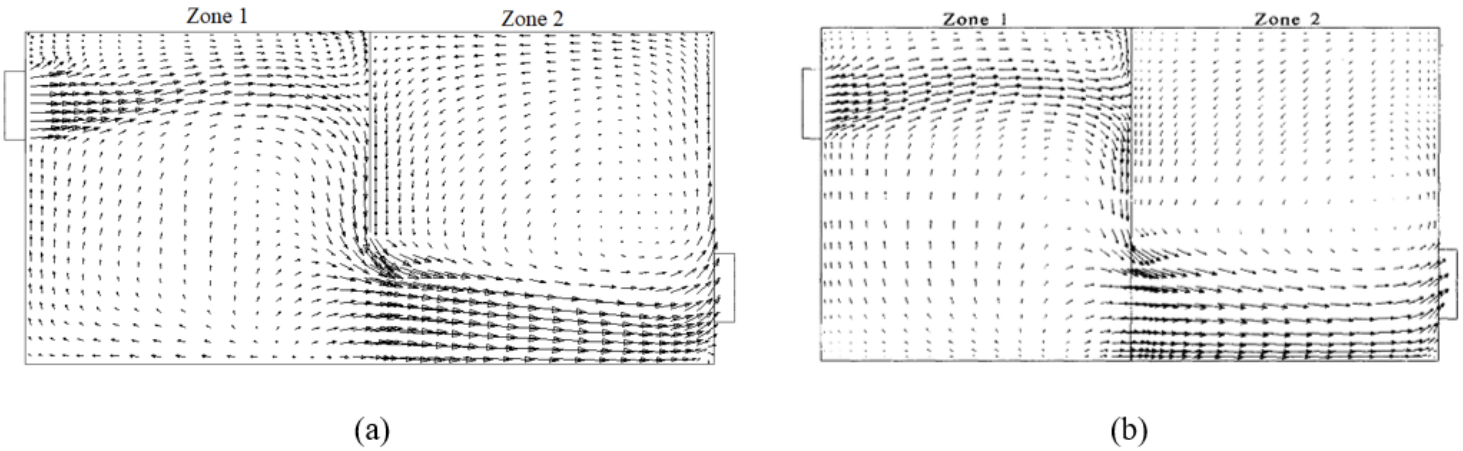

Figure 6

Comparison of airflow pattern in the centerline plane (width =1.5m) (a) present study (b) (Lu, W et al. 1996).

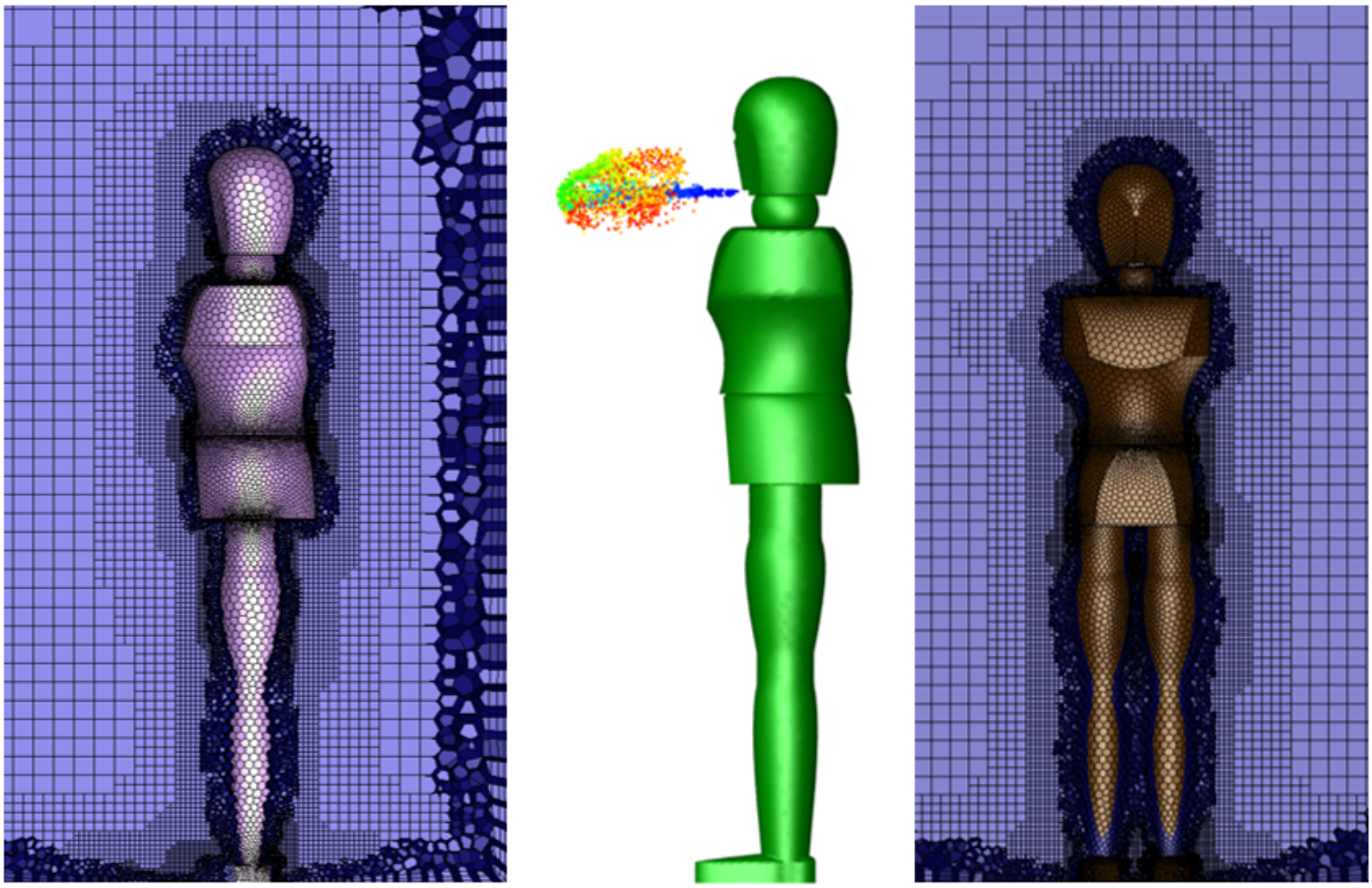

Figure 7

Mesh (poly-hexacore) structure used in the control room geometry.

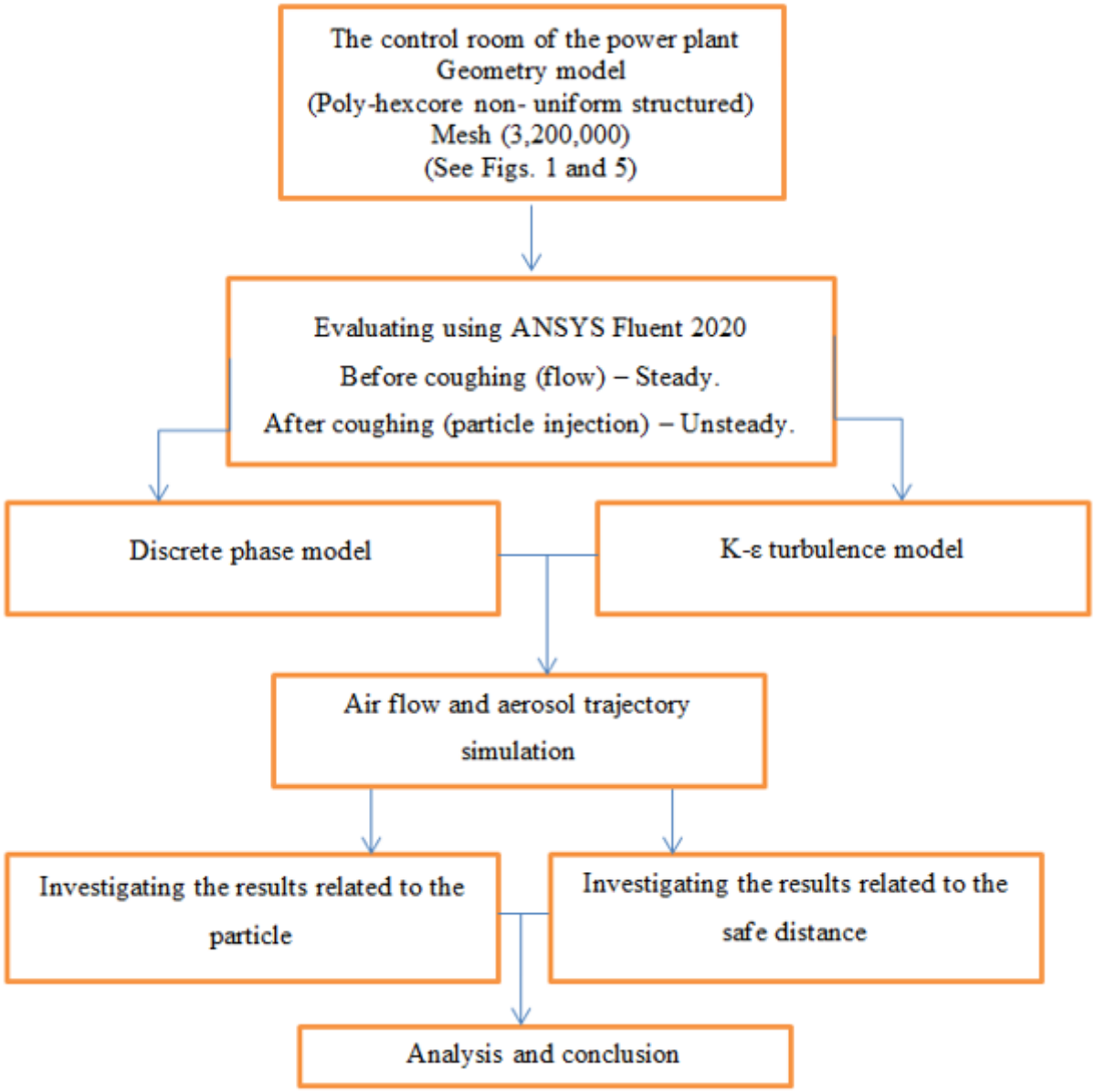

Figure 8

The procedure for the CFD modeling of the power plant control room.

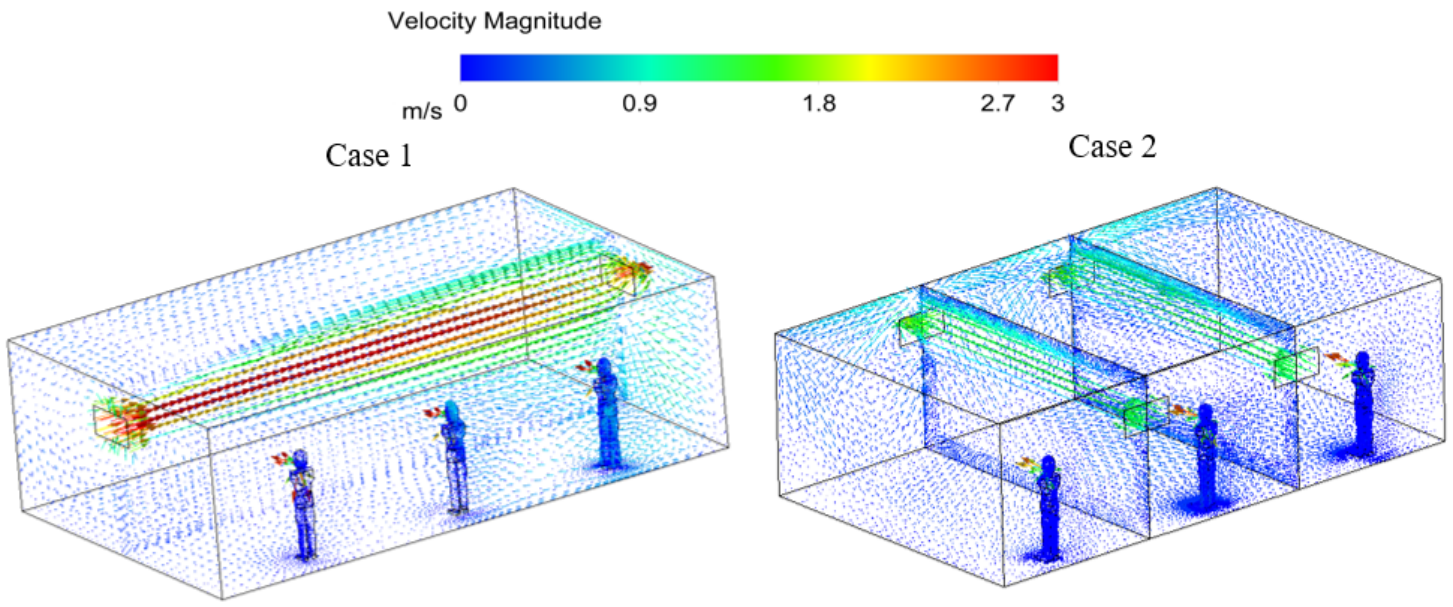

Figure 9

Velocity vector plots in the room at the mid-planes of the inlet-outlet registers and cough from the infected people's mouths.

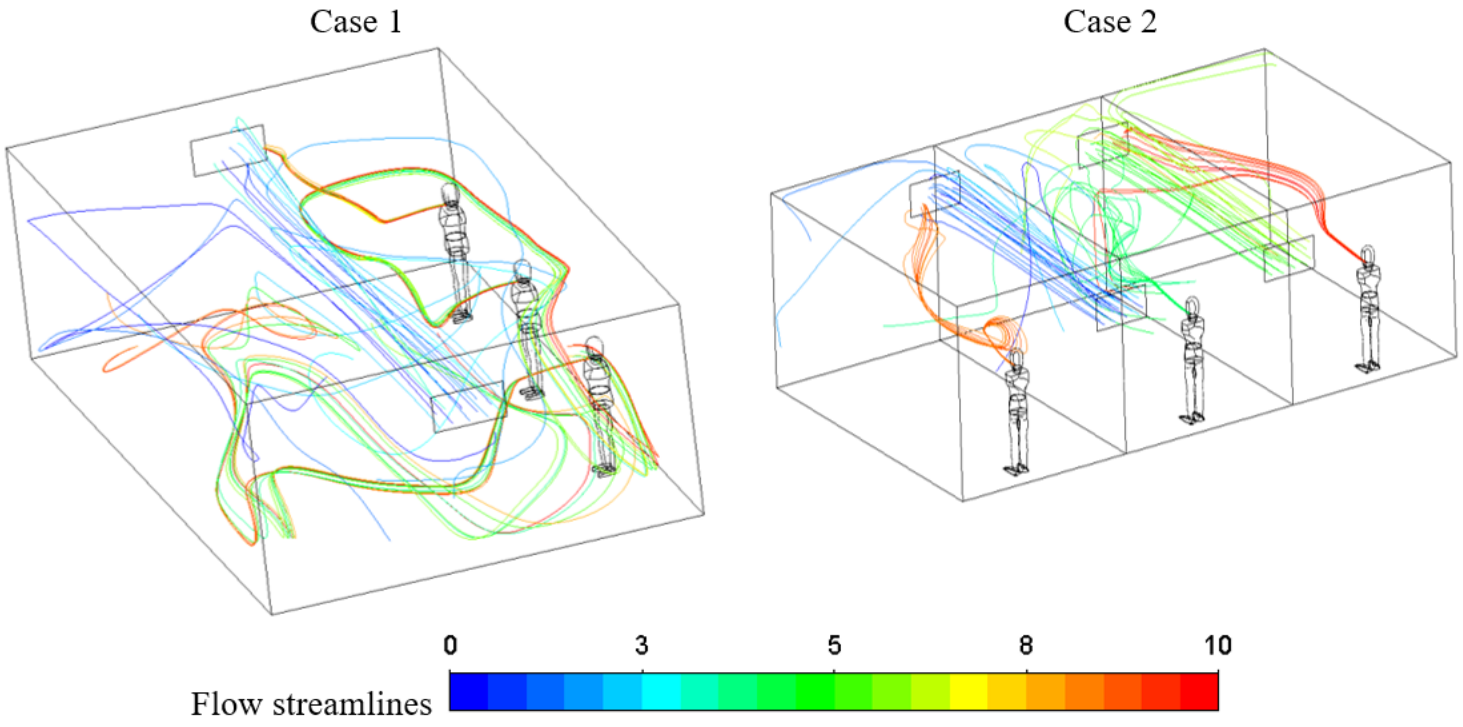

Figure 10

Airflow streamlines emerging from the ventilation inlets and cough flow from infected people's mouths.

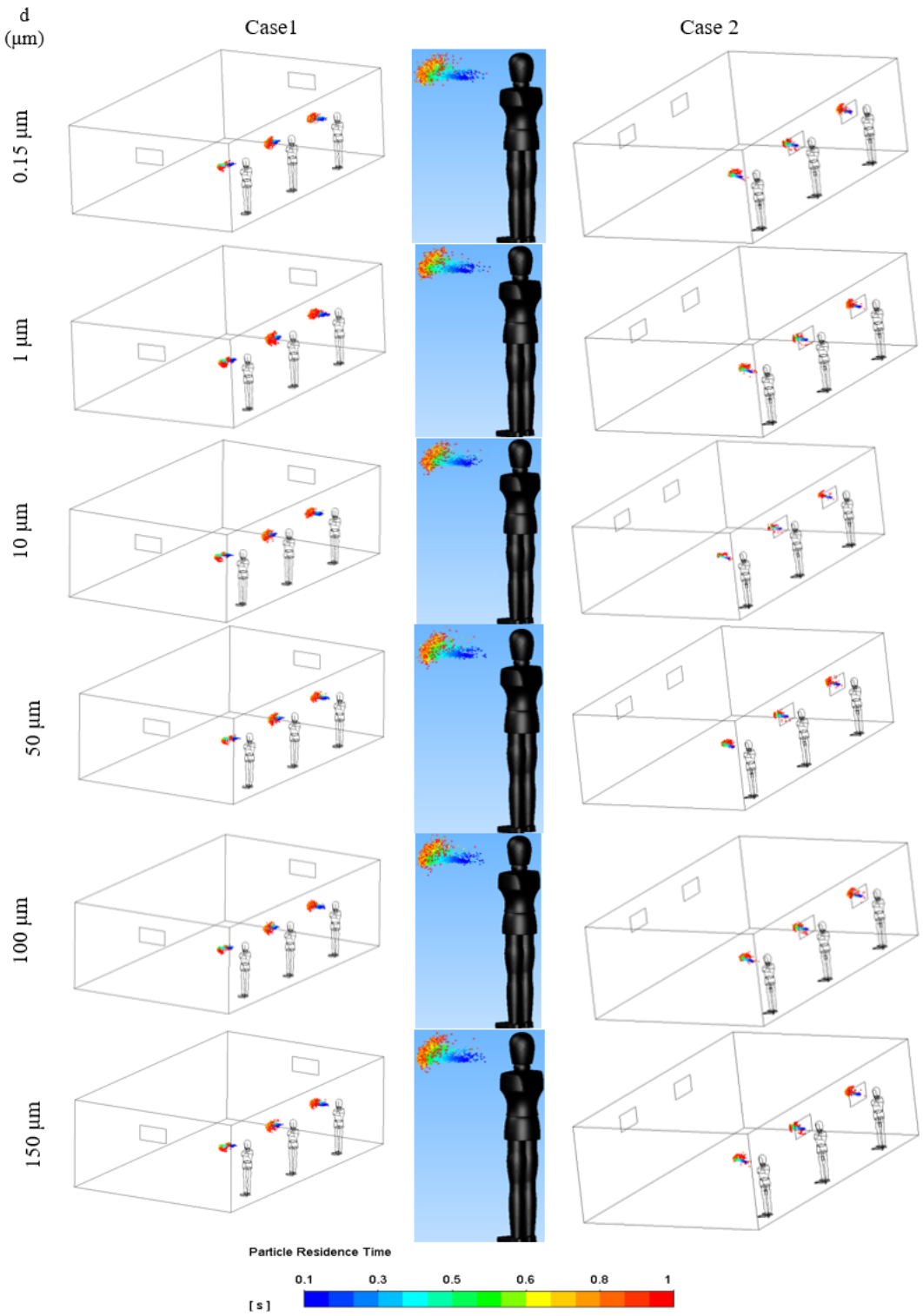

Figure 11

Respiratory droplet distribution at one second after coughing for different droplet diameters for a ventilation velocity of 10 m/s.

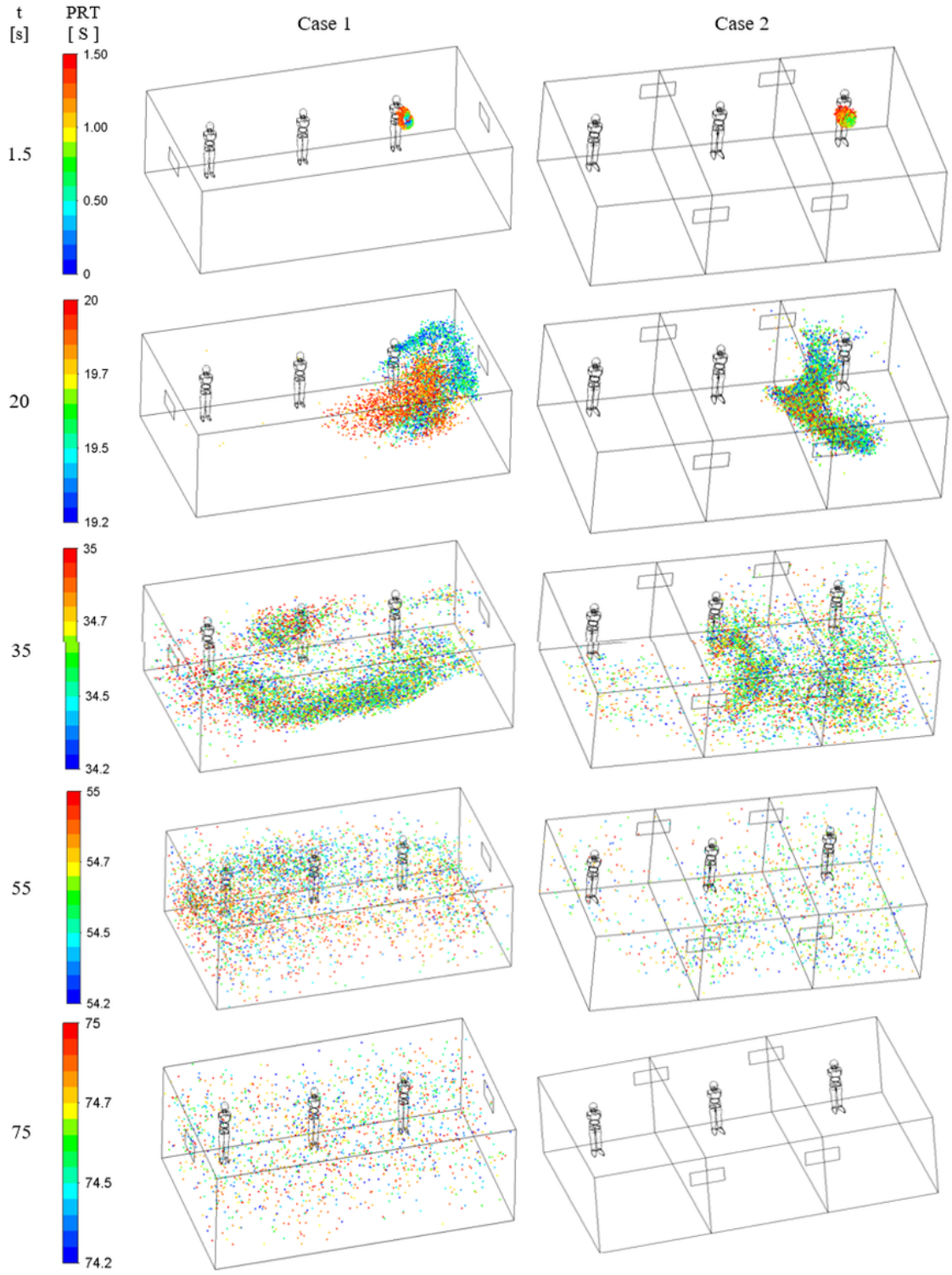

Figure 12

Respiratory droplet dispersion in the control room at different times for the cough emission from a person at location A for different ventilation systems (Case 1 and Case 2).

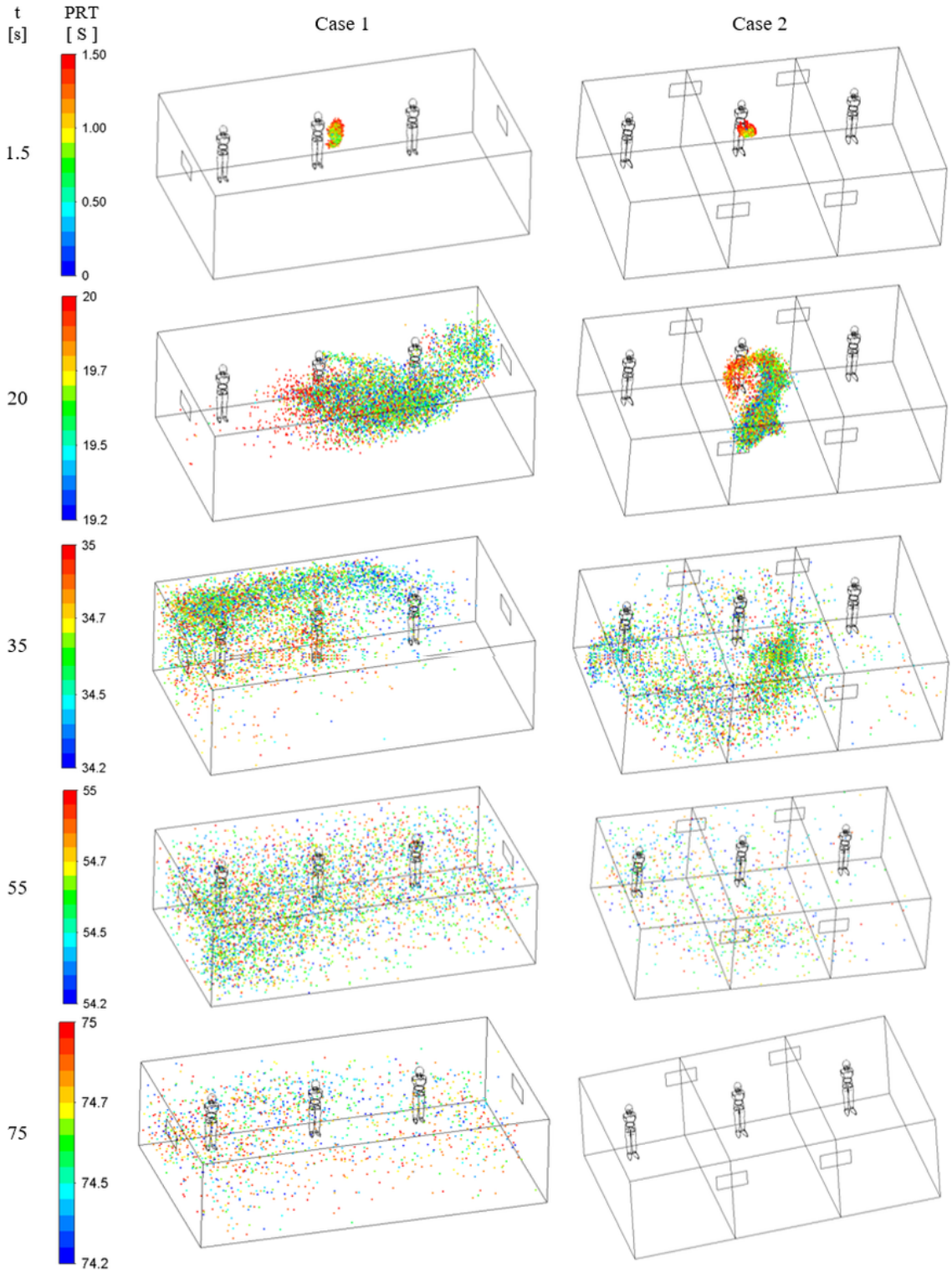

Figure 13

Respiratory droplet dispersion in the control room at different times for the cough emission from a person at location B for different ventilation systems (Case 1 and Case 2).

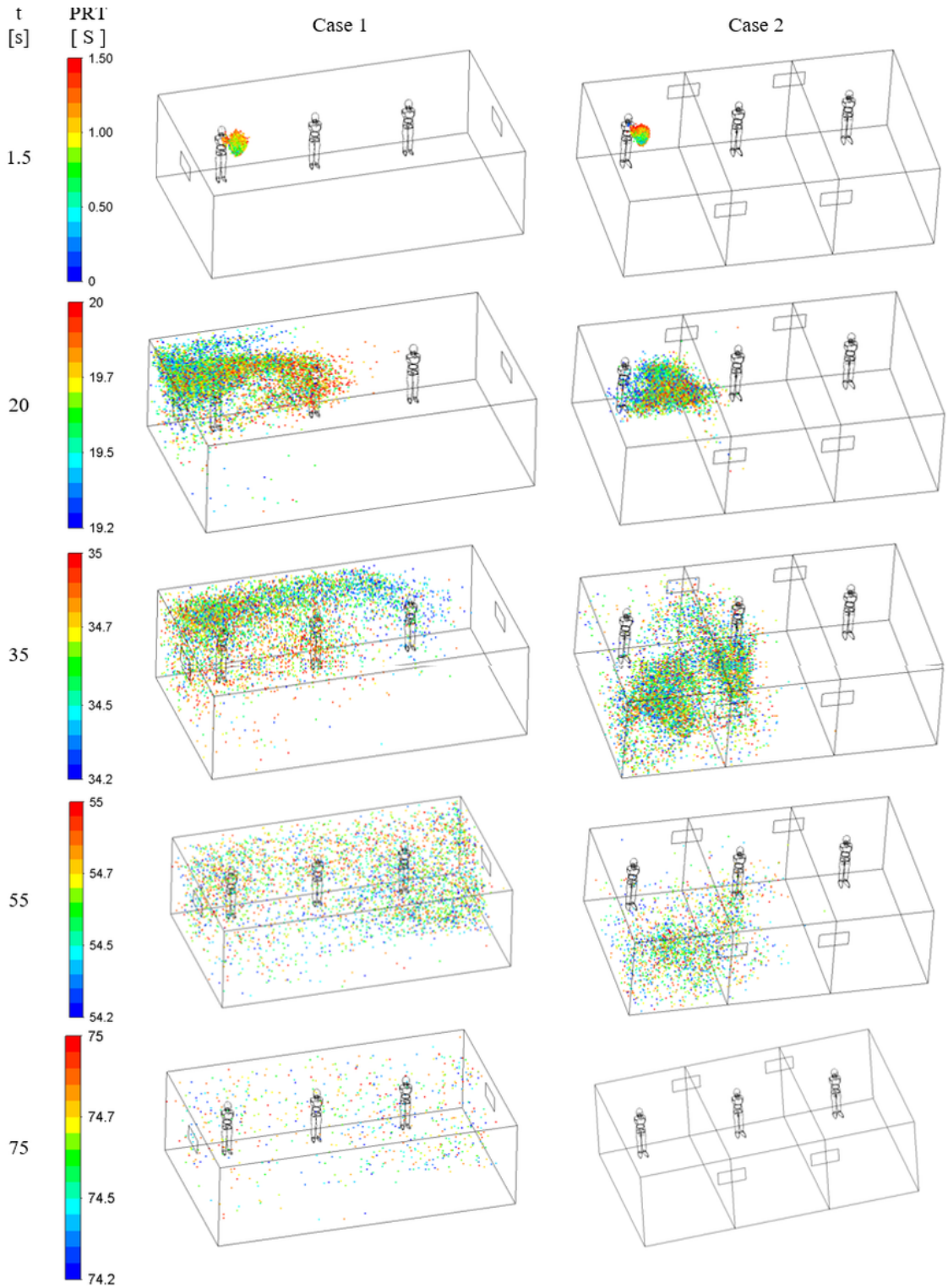

Figure 14

Respiratory droplet dispersion in the control room at different times for the cough emission from a person at location C for different ventilation systems (Case 1 and Case 2).

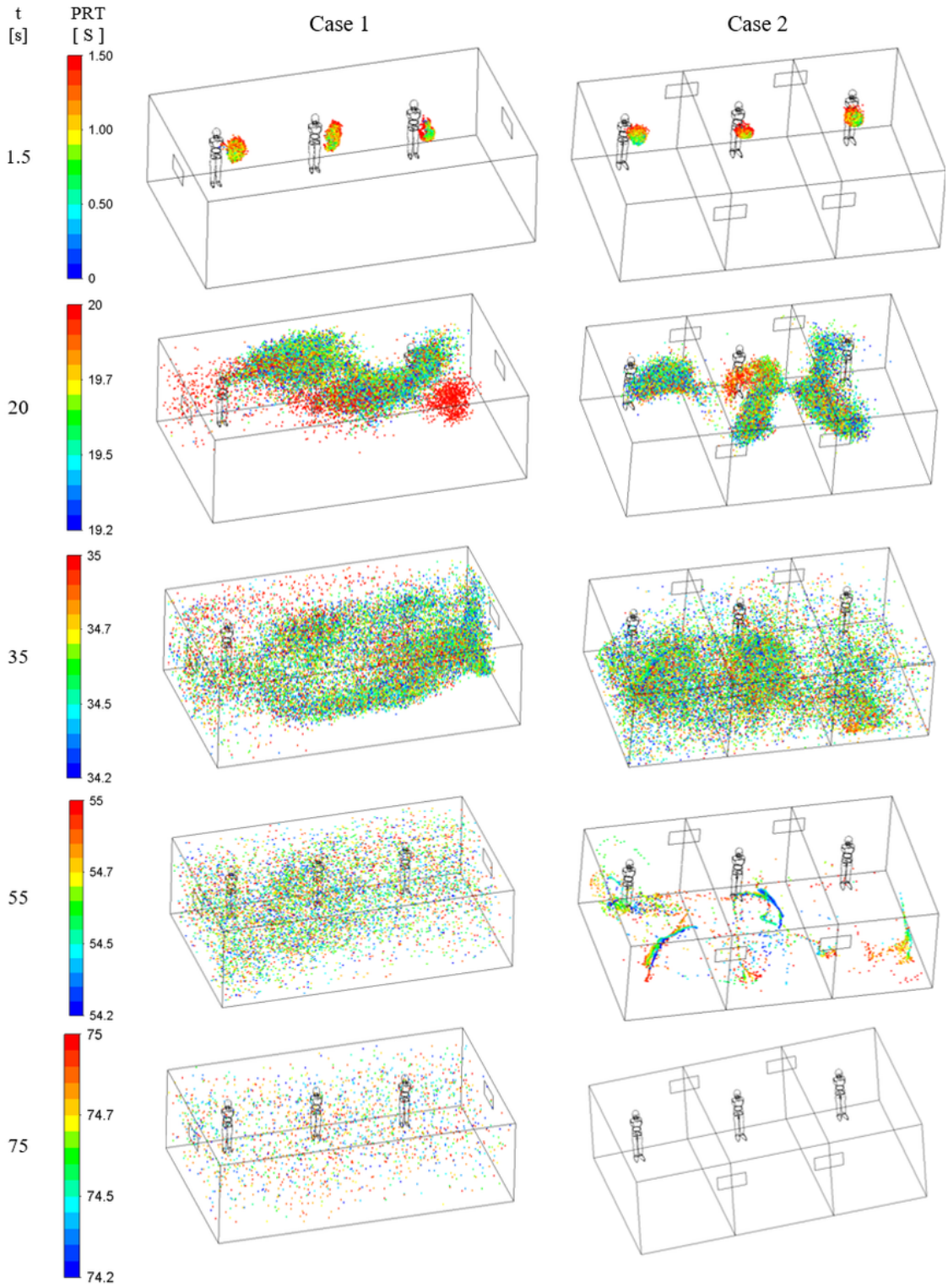

Figure 15

Respiratory droplet dispersion in the control room at different times for the simultaneous cough of three persons at locations A, B, and C for different ventilation systems (Case 1 and Case 2).

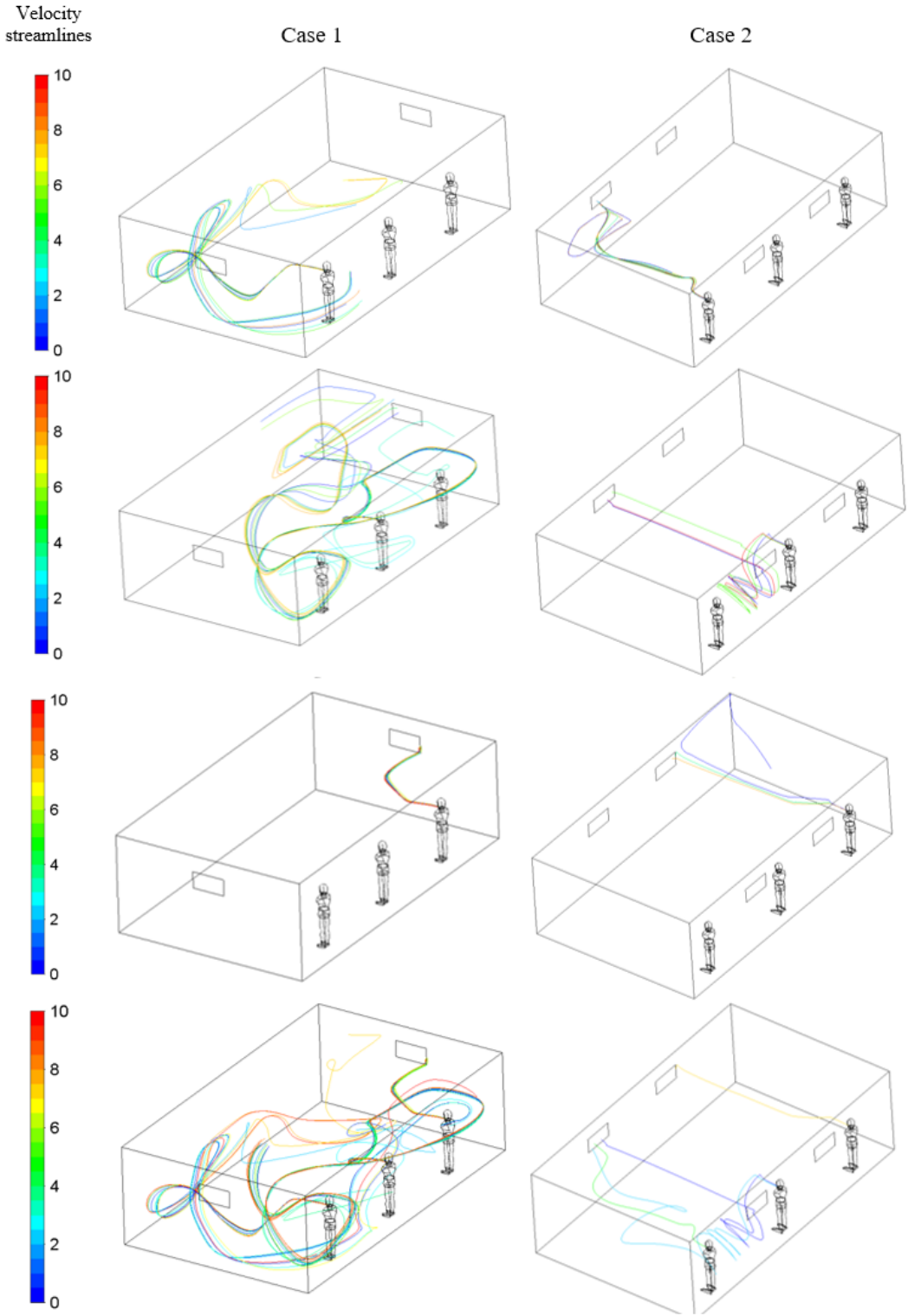

Figure 16

Airflow streamlines for the infected person coughing at different locations.

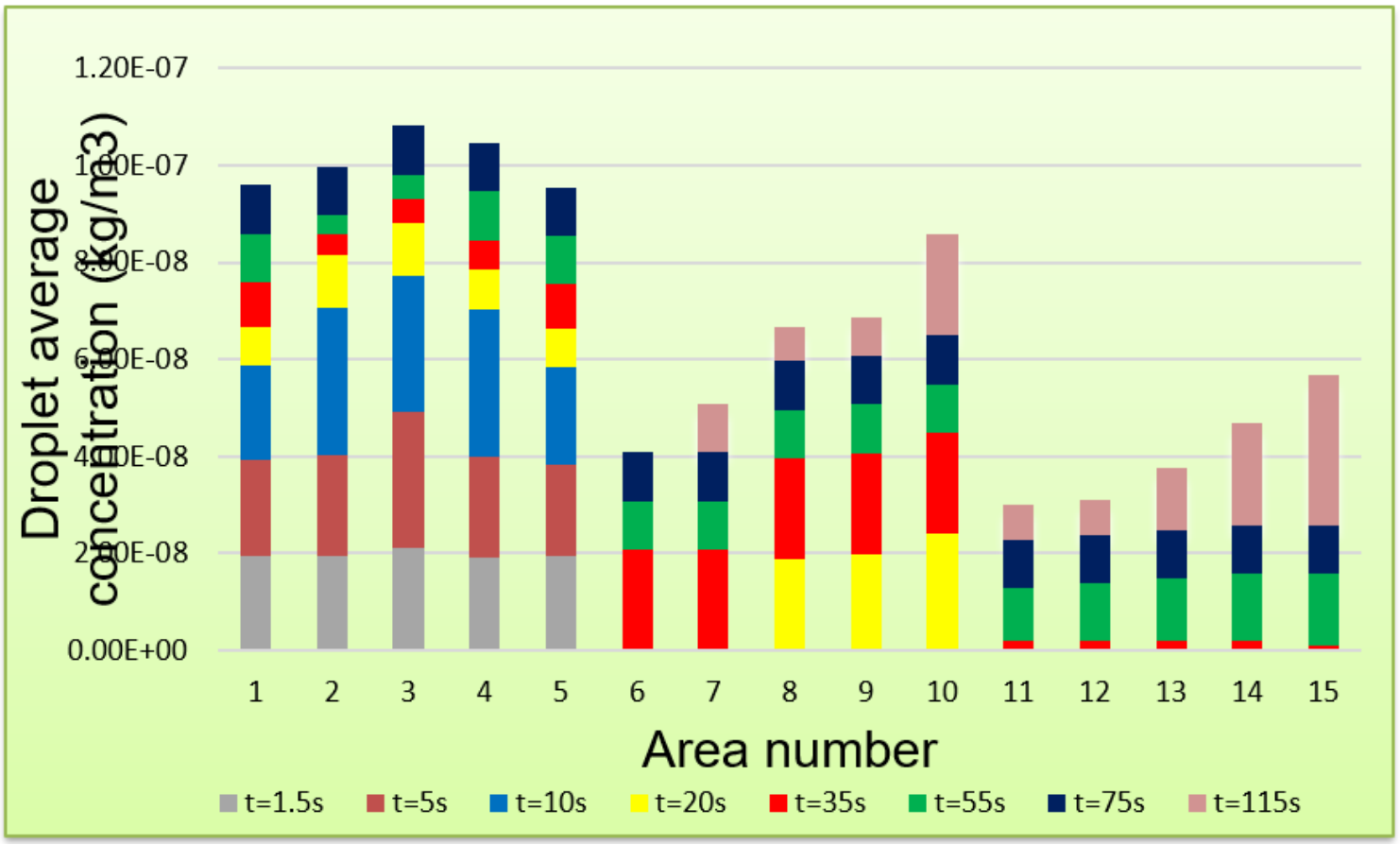

Figure 17

Average droplet concentration on the virtual plane (see Fig. 3 -Case 1) for each area at various times for the control room.

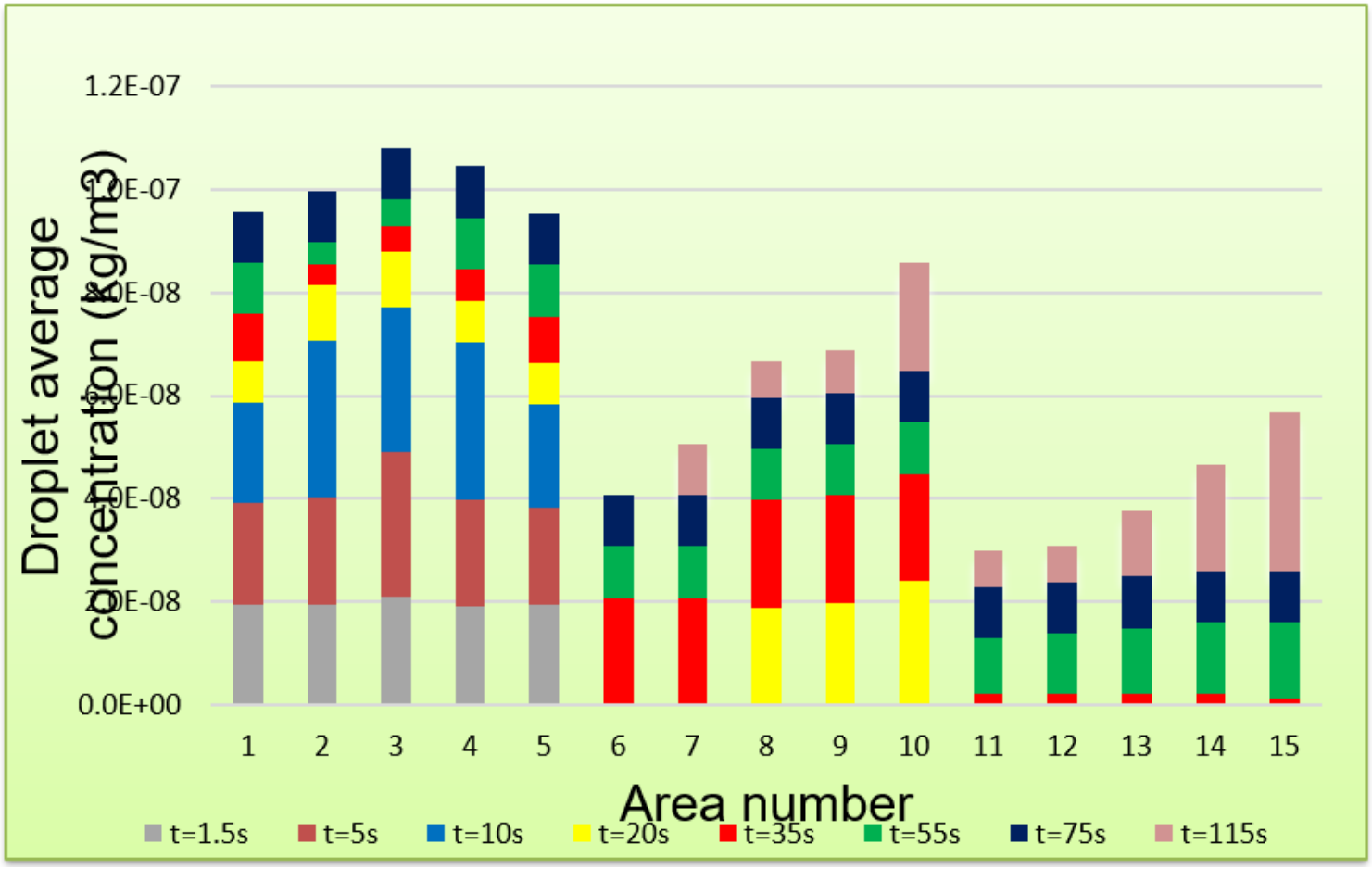

Figure 18

Average droplet concentration on the virtual plane (see Fig. 3-Case 2) for each area at various times for the control room.

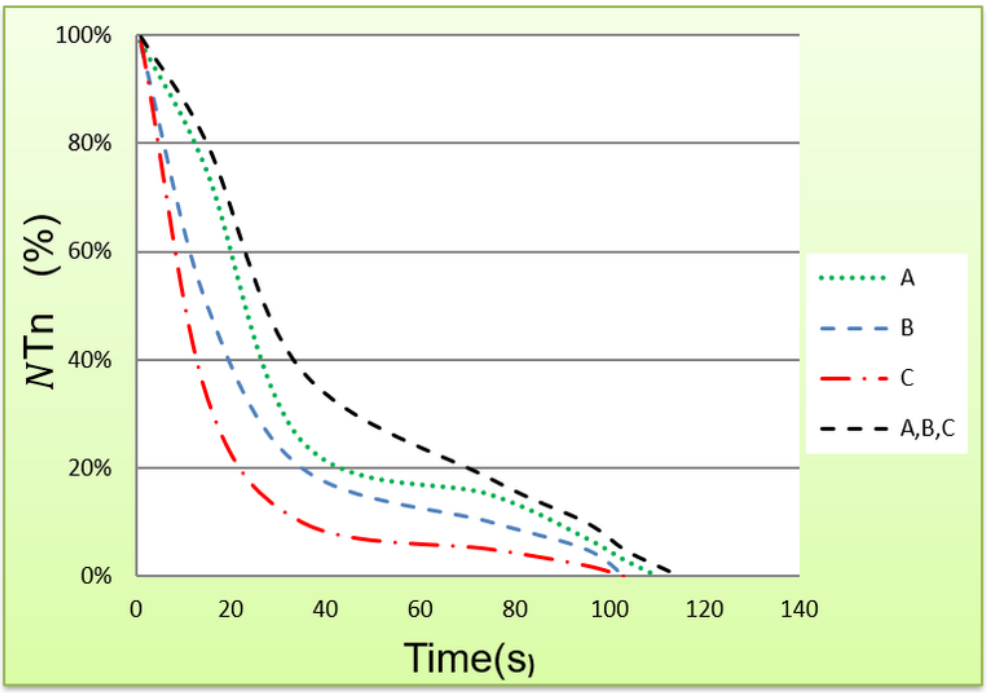

(a) Case 1

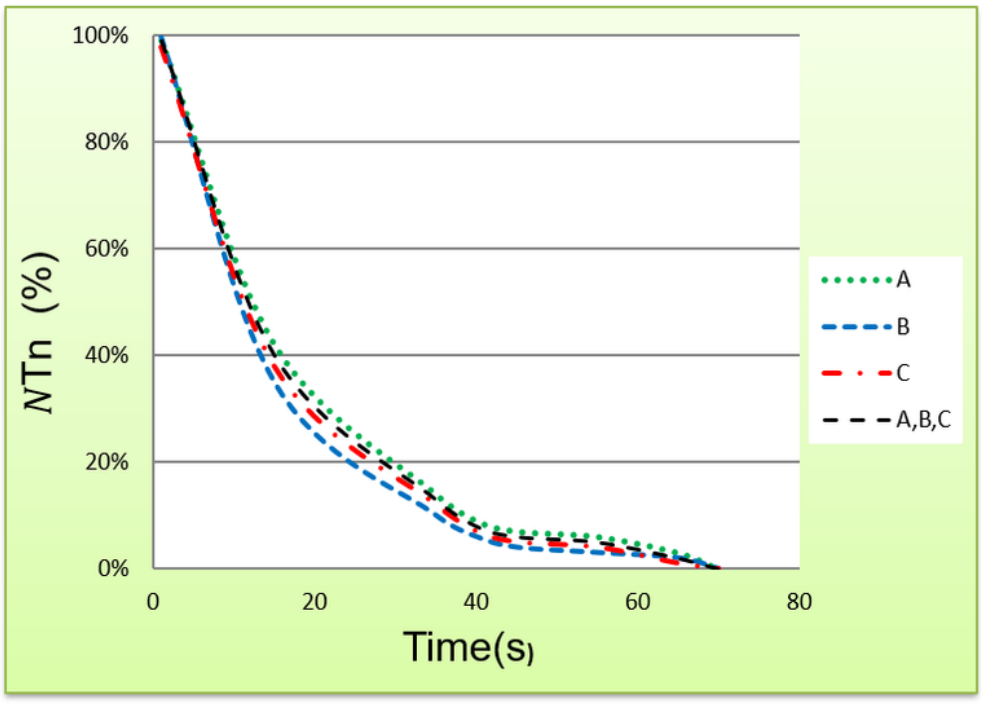

(b) Case 2

Figure 19

Time variation of the fraction of cough droplets remaining in the control room; (a) first ventilation system (Case 1) and (b) second ventilation system in (Case 2).